LABORATORY TESTING

OF THE

MAGNADRIVE

ADJUSTABLE-SPEED COUPLING SYSTEMS (ASCS)

A Report for the Northwest Energy Efficiency Alliance

By

Motor Systems Resource Facility
(MSRF)

Oregon State University

January 2000

LABORATORY TESTING OF THE MAGNADRIVE ADJUSTABLE-SPEED COUPLING SYSTEMS (ASCS)

List of Figures

18) Input Power for Flow Requirements for Fan Driven by Old 50 hp Motor
    a) Direct Drive and Output Baffles
    b) Drive Via ASCS
19) Input Power for Flow Requirements for Pump Driven by Old 50 hp Motor
    a) Direct Drive and Output Throttle Valve
    b) Drive Via ASCS
20) Temperature Rise of Shaft-End Bearing of Old 50 hp Motor Driving Fan Load
    a) Flow control by Baffles
    b) Flow Control by ASCS
21) Temperature Rise of Shaft-End Bearing of Old 50 hp Motor Driving Pump Load
    a) Flow Control by Throttle Valve
    b) Flow Control by ASCS
22) Temperature Rise of ASCS Discs Providing Fan Load from Old 50 hp Motor
    a) Magnet Disc Temperature Rise Above Ambient
    b) Conductor Disk Temperature Rise Above Ambient
23) Temperature Rise of ASCS Discs Providing Pump Load from Old 50 hp Motor
    a) Magnet Disc Temperature Rise Above Ambient
    b) Conductor Disk Temperature Rise Above Ambient
24) Input Power for Flow Requirements for Fan Driven by 100 hp Motor
    a) Direct Drive and Output Baffles
    b) Drive Via ASCS
25) Input Power for Flow Requirements for Pump Driven by 100 hp Motor
    a) Direct Drive and Output Throttle Valve
    b) Drive Via ASCS
26) Temperature Rise of Shaft-End Bearing of 100 hp Motor Driving Fan Load
    a) Flow Controlled by Baffles
    b) Flow Controlled by ASCS
27) Temperature Rise of Shaft-End Bearing of 100 hp Motor Driving Pump Load
    a) Flow Controlled by Throttling Valve
    b) Flow Controlled by ASCS
28) Temperature Rise of ASCS Discs Providing Fan Load from 100 hp Motor
    a) Magnet Disc Temperature Rise Above Ambient
    b) Conductor Disk Temperature Rise Above Ambient
29) Temperature Rise of ASCS Discs Providing Pump Load from 100 hp Motor
    a) Magnet Disc Temperature Rise Above Ambient
    b) Conductor Disk Temperature Rise Above Ambient
30) Input Power for Flow Requirements for Fan, Driven by 200 hp Motor
    a) Direct Drive and Output Baffles
    b) Drive Via ASCS
31) Input Power for Flow Requirements for Pump, Driven by 200 hp Motor
    a) Direct Drive and Output Throttling Valve
    b) Drive Via ASCS
32) Temperature Rise of Shaft-End Bearing of 200 hp Motor Driving Fan Load
    a) Flow Controlled by Baffles
    b) Flow Controlled by ASCS

33) Temperature Rise of Shaft-End Bearing of 200 hp Motor Driving Pump Load
    a) Flow Controlled by Throttling Valve
    b) Flow Controlled by ASCS
34) Temperature Rise of 200 hp ASCS Magnet Discs
    a) Fan Load
    b) Pump Load
35) Temperature Rise of 200 hp ASCS Conductor Discs
    a) Fan Load
    b) Pump Load
36) Photographs of 200 hp ASCS
    a) Differences in Magnet Disc to Conductor Disc Clearances
    b) Loss of Paint Due to Overheating of Conductor Disc
37) Temperature Rise of 200 hp ASCS Conductor Disc Driving Pump Load
    a) Without Cooling Fins
    b) With Cooling Fins
38) Comparison of Starting Currents of 200hp Motor
    (a) Continually Coupled to Dynamometer
    (b) Initially Decoupled from Dynamometer
39) Conventional Variable Frequency Drive (VFD) System.
40) Input Power for Flow Requirements for Fan Driven by New 50 hp Motor
    a) Direct Drive and Output Baffles
    b) Drive Via 50kVA VFD
41) Input Power for Flow Requirements for Pump Driven by New 50hp Motor
    a) Direct Drive and Output Throttle Drive
    b) Drive Via 50kVA VFD
42) Input Voltage and Current of VFD with New 50hp Motor at 201N and 1697 r/min
43) Input Power for Flow Requirements for Fan Driven by Old 50 hp Motor
    a) Direct Drive and Output Baffles
    b) Drive Via 50kVA VFD
44) Input Power for Flow Requirements for Pump Driven by Old 50 hp Motor
    a) Direct Drive and Output Throttle Valve
    b) Drive Via 50kVA VFD
45) Input Power for Flow Requirements for Fan Driven by 100 hp Motor
    a) Direct Drive and Output Baffles
    b) Drive Via 100kVA VFD
46) Input Power for Flow Requirements for Pump Driven by 100 hp Motor
    a) Direct Drive and Output Throttle Valve
    b) Drive Via 100kVA VFD
47) Input Power for Flow Requirements for Fan, Driven by 200 hp Motor
    a) Direct Drive and Output Baffles
    b) Drive Via 250kVA VFD
48) Input Power for Flow Requirements for Pump, Driven by 200 hp Motor
    a) Direct Drive and Output Throttling Valve
    b) Drive Via 250kVA VFD

List of Tables

Executive Summary

Background

The value of adjustable speed control in industrial applications is well proven by the increasing number of installations in which induction motors are powered by variable frequency drives (VFD's). Adjustable speed drives can provide energy savings and improve process control. This is especially true for systems such as fans and pumps where flow control is achieved by baffles and valves. However, VFD's have drawbacks including: high purchase and installation costs, motor bearing pitting, insulation failure, electromagnetic interference with control and measurement equipment, harmonic distortion generation, and tripping due to power disturbances. The correction of these problems requires additional equipment and techniques which further increase the capital cost. This provides an opportunity for an adjustable speed system of relatively low cost, which is robust and easy to use, and produces no adverse effects in the motor or power supply. The MagnaDrive adjustable speed coupling may have the potential to meet this opportunity. The MagnaDrive Coupling uses eddy-currents produced by rare earth magnets to transmit torque across the coupling. Varying the width of the air gap within the coupling controls the torque transmitted, thus permitting speed control.

Test Program

Three MagnaDrive Couplings rated at 50hp, 100hp, and 200hp; and three VFD's rated at 50kVA, 100kVA and 250kVA, were tested providing adjustable speed to achieve flow control. They were compared to direct-coupled pump and fan installations using throttling or baffling to achieve flow control. All systems were evaluated for flow control capability, power consumption, power factor, total harmonic distortion (THD), vibration, noise, and temperature changes.

Methodology

The operating characteristics of a centrifugal fan and a low-head centrifugal pump were determined on Oregon State University's Motor Systems Resource Facility's (MSRF) laboratory dynamometer. The pump and fan were evaluated in two flow control modes: variable speed operation; and constant speed with throttling or baffling flow control. The flow, speed and torque characteristics of the pump and fan tested were then extrapolated to provide system characteristics at the 50, 100 and 200 hp levels.

MagnaDrive Couplings were connected to 50hp, 100hp and 200hp 60hz direct on-line induction motors. These drove the laboratory dynamometer programmed with variable speed pump and fan characteristics. The test units were stepped through the complete flow ranges, data being taken once thermal stability at each test point was attained. The dynamometer tests were repeated using VFD's to control the motor speed. Finally, the tests were repeated with the motors directly coupled to the dynamometer, which was programmed with the throttled pump and baffled fan characteristics.

Results

The MagnaDrive Couplings provided complete and stable speed control operations from standstill to a little below the full-load speed of the induction motor.

The MagnaDrive Couplings are far more process energy efficient than baffled fans, up to 30% improvement; and throttled pumps, up to 44% improvement, depending on operating speed. The energy savings for a specific installation can be quantified if the system flow requirements are known. The MagnaDrive Coupling achieves an average of 62% of the VFD energy savings for fans, and 65% of the VFD savings for pumps.

Speed control by the MagnaDrive ASCS coupling is obtained at the expense of energy dissipation. The energy dissipation is evidenced by a temperature rise in the coupling.

The total harmonic distortions (THD) produced by the MagnaDrive coupled motors are excellent when compared to VFD controlled motors, and are very similar to directly connected motors. The power factor of the MagnaDrive-coupled motor is higher than the VFD driven motor for the upper half of the flow range, but lower than directly connected motors (although readily correctable).

The acoustic noise levels of the MagnaDrive Coupling are higher than the VFD, and are associated with the windage of the coupling. Vibration levels of the MagnaDrive Coupling were similar to the VFD and direct-coupled units tested, and never exceeded 0.050 IPS in any direction. The MagnaDrive Coupling is not a source of torque pulsations.

Motor bearing temperatures run cooler at low flow rates on the MagnaDrive-coupled systems than either VFD or throttled/baffled systems, and are similar at high flow rates.

The starting current characteristics of a MagnaDrive-coupled motor are changed, because the load is decoupled from the motor during starting. The inrush duration was reduced from 20 milliseconds to 10 milliseconds in the 200hp system test.

Conclusions

The tests demonstrated the viability of the principal of the MagnaDrive Coupling as a simple, non-electronic, adjustable speed drive. These couplings offer the ability to provide speed control to processes driven by constant speed motors.

The MagnaDrive Coupling provides substantial energy efficiency improvements over baffled fan or throttled pump operations. Although the energy efficiency of the MagnaDrive coupled system is less than the VFD system, a complete analysis of purchase and installation costs, and other operating benefits is required before a valid economic comparison can be made.

The lack of THD, and the insensitivity of a MagnaDrive-coupled system to poor power quality make the MagnaDrive Coupling appealing where power quality is a major concern.

This study has focused on centrifugal-type loads where the torque decreases rapidly with speed. The MagnaDrive Coupling should be evaluated with other types of loads, such as high-head pumps, or constant torque loads. The thermal characteristics of the coupling should be investigated, as it appeared to be sensitive to the load type and the power rating.

1. Introduction

Recent surveys [1] indicate that fans/blowers and pumps comprise 42% of all industrial loads by energy consumption, which accounted for some 250 billion kilowatt-hours in the USA in 1990. Consequently it is important to perform these functions as efficiently as possible. However, the traditional means of regulating the flow from these loads, respectively by throttling valves for pumps and baffling vanes for fans, are well known to be inefficient. The wasted energy is dissipated as heat in the throttling systems and the fluids being circulated in the industrial processes. Over the past 20 years, power-electronic adjustable-speed, or variable-frequency, drives (VFDs) have been introduced in increasing numbers to provide a high-efficiency alternative means of control by matching the output torque and speed of induction motors to the requirements of the loads. However, the energy savings resulting from the introduction of VFDs are obtained at the cost of significant capital expenditure: VFDs are generally much more expensive than the induction motors they control, and the cost of installation and environmental provisions for the VFD, must be factored into the overall cost/benefit equations. For example, the average cost for 100kVA VFDs is about $6,800 ($68/kVA), for 50kVA drives is about $4,000 ($80/kVA), and motors in this range run about $40/hp for industrial totally enclosed fan cooled motors, and $30/hp for drip proof motors for office/commercial installations. In Europe and Japan, where energy costs are substantially higher than in the USA, VFDs have been installed in far greater percentage numbers. According to a study conducted by the Ducker Worldwide research company in 1999, the VFD market penetration (i.e. the percentage of motors being driven by VFDs) in the USA is 18% in currently sold systems and 12% in existing installations, in Europe 24% sold and 19% installed and finally in Japan 45% sold and 38% installed. Often in the USA, VFD's are reputed to be justified on the basis of improved process control rather than energy savings alone [2].

In addition to their relatively high capital cost, VFDs have experienced technical impediments to their introduction and adoption by industry. Early model of VFDs suffered reliability problems. These forced plant designers/operators to retain the

throttles/baffles and to install VFD by-pass switches to ensure uninterrupted processes. This compounded the capital and installation payback problem. Advances in power electronic devices have helped reduce the reliability issues of VFDs. Thyristors and bipolar junction transistors (BJT) have been replaced by insulated gate bipolar transistors (IGBT) and power MOSFETs. These advanced devices have reduced VFD circuit complexity and have improved the performance by use of higher device switching speeds. The latter benefit for the VFD has, in certain cases, produced operational problems in the induction motors [3]. These problems include: increased stress of motor insulation, especially for smaller motors connected via long cable lengths; common-mode voltage effects leading to capacitively induced motor shaft voltages and resulting bearing currents; both radiated and conducted electromagnetic interference (EMI); high harmonic content of the currents drawn from the supply, particularly at low load levels. Effective solutions have been developed to all of those problems [3], but these solutions generally require additional equipment, thus increasing the complexity and cost of the system.

An alternative means of matching motor outputs to their industrial loads is by means of a permanent-magnet eddy-current coupling. In these devices, sets of alternately polarized, axially-orientated, magnets are rotated close to a disc of conducting material. The relative speed, between magnets and the conducting disc, or slip, causes eddy currents to be induced in the conductor. These currents enable the transmission of torque, across the airgap between magnets and conductor, without mechanical contact. Controllable versions of eddy-current couplings have been developed using electromagnets operating with controlled excitation currents to provide the required magnetic field strengths. However, these do not compare at all favorably with VFDs for overall energy efficiency, partially due to the excitation losses of the electromagnets, in addition to the slip energy losses in the conductor discs, which will be discussed below.

Considerable recent attention has been dedicated to the use of the newer high energy-product permanent magnets (PM) based on the rare-earth metal neodymium. Magnets of the alloy neodymium/iron/boron (Ne/Fe/B) have high magnetic field strength,

support good flux density, and have low losses. This development in materials has produced new ranges of both dc and ac electric motors and an eddy-current coupling. Early prototype forms of PM eddy-current couplings have been evaluated in Oregon State University [5,6]. From these early prototypes, commercial products have been developed and recently a technique for analysis and performance prediction has been published [8]. The proposed advantages of this coupling include:

(i) mechanical isolation of motor and load – this enables soft-starts, a certain tolerance for misalignment of motor and load shafts, while providing a "cushion" for the motor to vibrations and disturbances originating in the load;
(ii) electrical isolation – this can prevent the circulation of ground currents which affect instrumentation and also the transmitting of shaft voltages which may produce harmful bearing currents.
(iii) Thermal isolation.

In order to provide the facility of control to a permanent-magnet coupling, it is necessary to be able to adjust the rate of change of magnetic flux linkage of the conduction disc. One way of doing this is to increase or decrease the radius at which the magnets are positioned. However, for an adjustable coupling, this will result in poor overall utilization of conductor material.

During the study of fixed gap couplings [5,6] the effects of different settings for the clearance between magnets and conductor disc were investigated. This demonstrated the electromagnetic viability of this alternative, provided that a sound technique could be developed for the mechanical control of the clearance. This technique is employed in the adjustable speed coupling system (ASCS) which is the subject of the present study.

The electromagnet components of the ASCS are shown schematically in Fig. 1. Two composite discs, steel backed (for magnetic circuit continuity as well as structural requirements) with copper faces, are tied together via spacers and rotate with the motor shaft. Between these, two axially moveable aluminum discs support arrays of axially

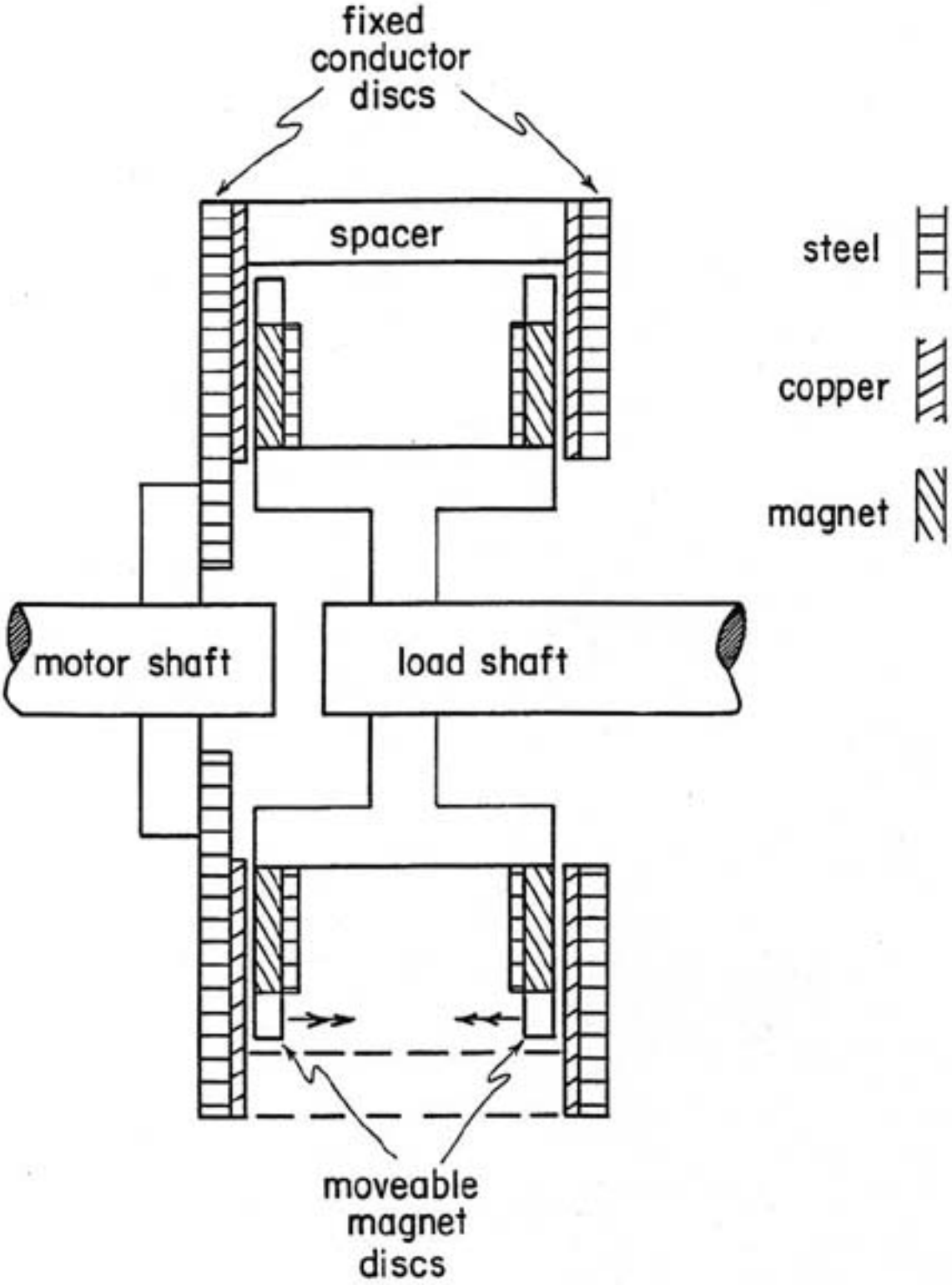

Fig. 1 Mechanical Schematic of Adjustable Speed Coupling System (ASCS)

orientated NeFeB permanent magnets with alternating polarities. For the position of minimum mechanical clearance between the magnet discs and the conductor discs, the flux density produced by the magnets is a maximum. As this clearance increases, so does the reluctance of the magnetic circuit, with the result that the magnetic flux decreases. It is the combination of magnetic flux and the relative motion of the conductor discs and magnet discs that induces currents in the former. In turn the induced currents result in torque production. Theoretically the magnetic couplings, both fixed gap and adjustable, are torque transmitting devices: i.e. the torque on the magnet discs equals the torque on the conductor discs regardless of the slip between them. This was demonstrated to be true in the previous study [5] provided allowance is made for losses such as bearing friction and windage in the device. As torque is directly related to magnetic flux, it is to be expected that the torque produced by the ASCS is inversely proportional to the clearance.

Fig. 2 shows the measured torque of the nominally 200hp rated ASCS, as a function of clearance. For a clearance above 11mm the expected inverse proportionality is evident. At smaller clearances than this, the torque does not increase as predicted indicating significant saturation of the magnetic circuit. When the ASCS is employed to drive a load, its operation is dictated by two factors: the slip between conductor and magnet discs and the power required by the load at a particular speed. The simple linear relationship between slip and load speed is given in Fig. 3a. The ASCS, being inherently an induction type device, incurs losses in its secondary (the conductor disc) that are directly proportional to the slip and the load (power) being transmitted.

The centrifugal device characteristic is shown in Fig 3b, in which torque is proportional to the square of speed, and power is proportional to the cube. Consequently, the losses due to this load type can be calculated directly as the product of Figs 3a and 3b. The results of this product are shown in Fig 3c. For these centrifugal fan and pump loads, the peak loss requirement is 10.55% of the rating, which occurs at 75% speed. The

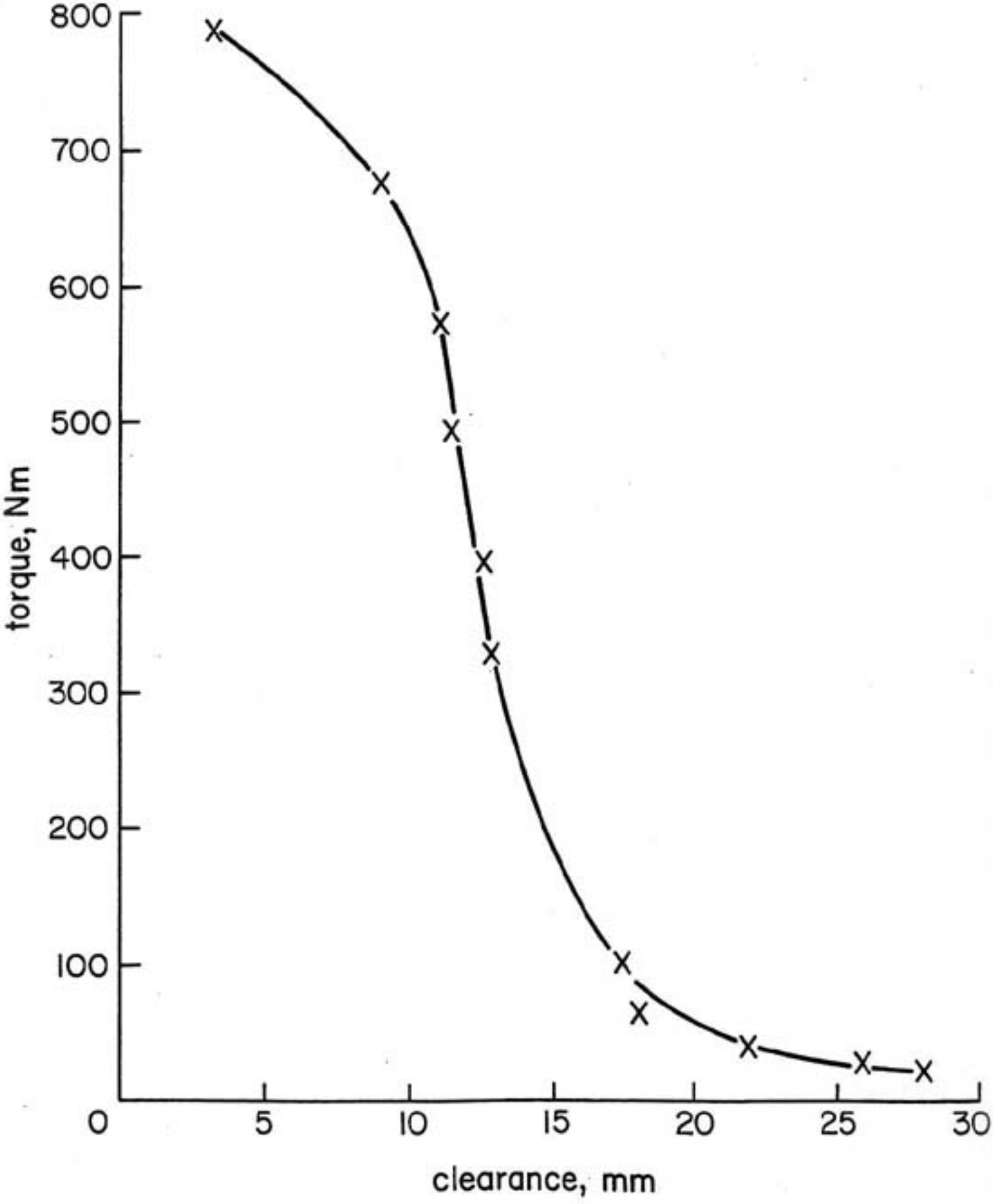

Fig. 2 Measured Torque as Function of Clearance for 200 hp ASCS

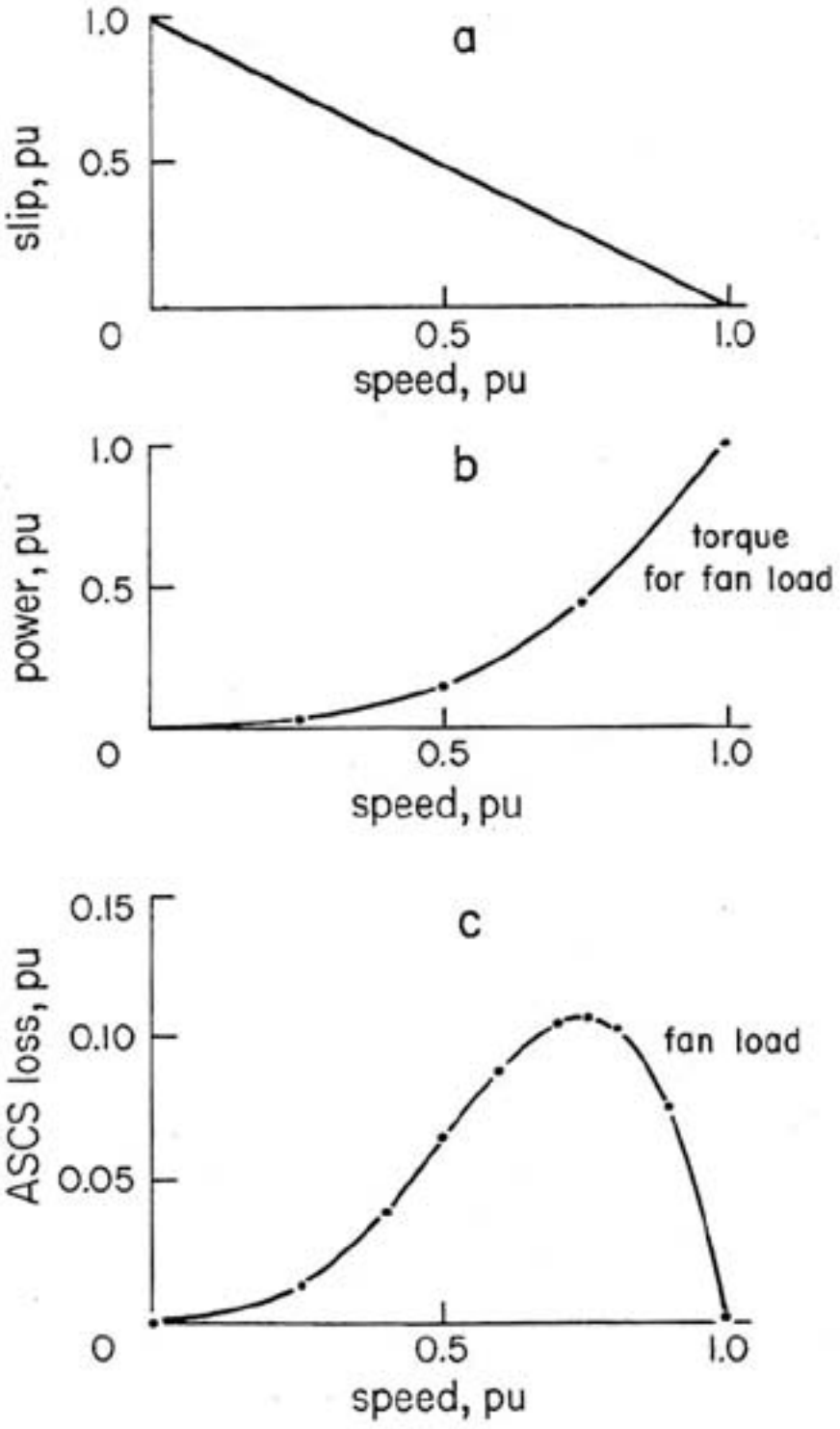

Fig. 3 Theoretical Estimate of ASCS Losses for Centrifugal Loads
a) Slip
b) Load Power Transmitted
c) Resulting Losses

basis for extending this analysis to loads other than the pure centrifugal type is given in Sections 6.3.2 and 6.3.3.

The test program described in Sections 4 and 5 of this report has measured the significant operation features of the three methods of controlling the flow rate of both fans and pumps, as shown schematically in Fig. 4, namely throttling, adjustable speed by a VFD, and adjustable speed by ASCS.

2. The MSRF Test Platform

The tests conducted in this study have taken place in the Motor Systems Resource Facility (MSRF), a laboratory in the Electrical and Computer Engineering Department at Oregon State University (OSU). A schematic of the laboratory power system is given in Fig. 5. For the range of tests required in this project, 50hp, 100hp and 200hp, the larger test bed rated up to 300hp was used.

The heart of the 300hp test bed is its bidirectional, fully regenerative dynamometer system comprised of an induction machine and a four-quadrant inverter. Details of these components are given in Section 9.A.1. Full four-quadrant capability allowed the dyno to operate (i) as a drive, as described in Section 3.1, to characterize the loads such as the fan and (ii) as a load to simulate fans and pumps with a high degree of control. The torque and speed (and hence, power) of the dynamometer were measured by a non-contact shaft transducer, employing strain gauges (for torque) and an inductive pick-up (for speed). Details of the torque-speed measurement system are given in Section 9.A.2. To ensure end-to-end accuracy of the measurements, the torque transducers were calibrated by attaching known masses to known torque arms. Two torque transducers were employed to ensure best use of the scale. Speed signals were measured by a Phillips PM6666 pulse counter to provide the quoted accuracy.

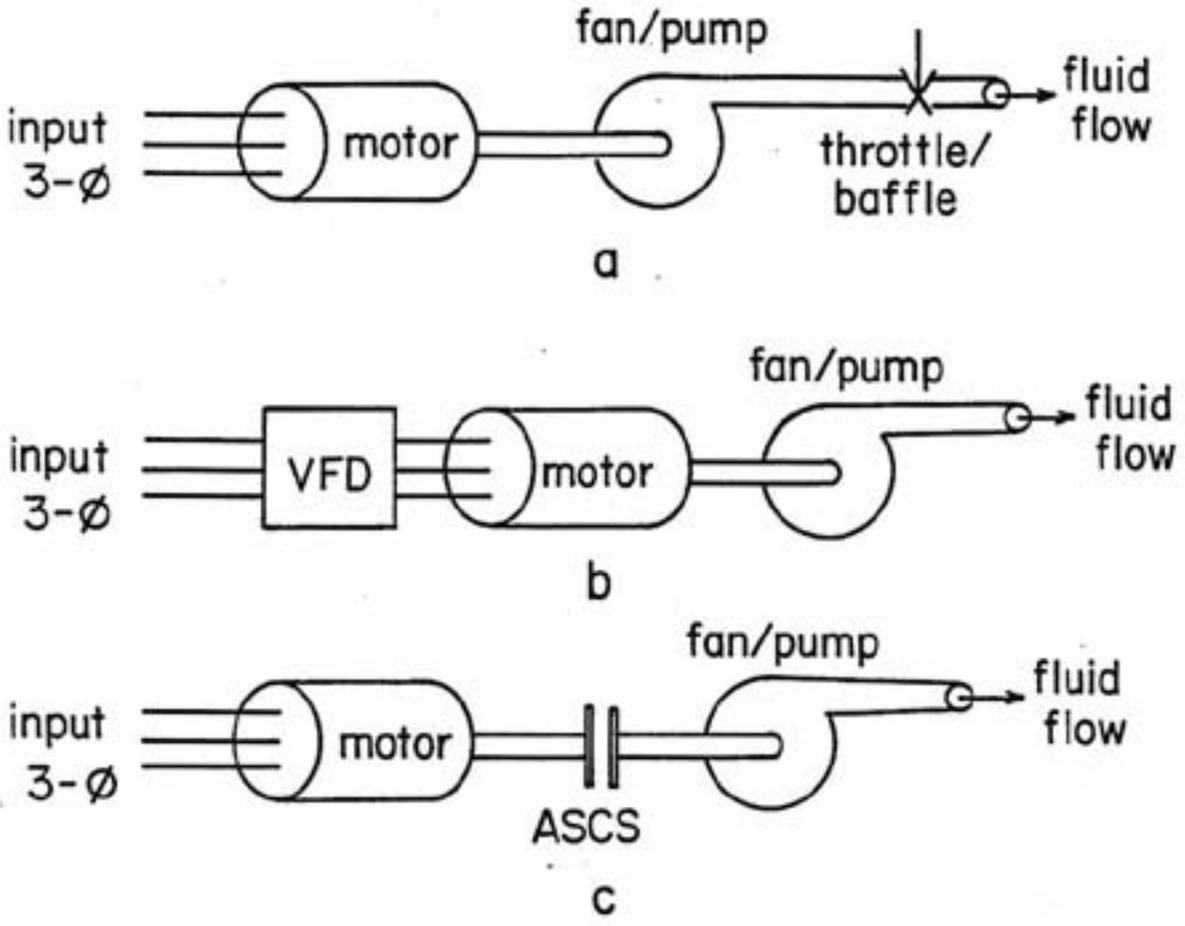

Fig. 4 Alternative Methods of Fluid Flow Control
a) Throttling
b) Motor Speed Adjustment
c) Adjustable Speed Coupling

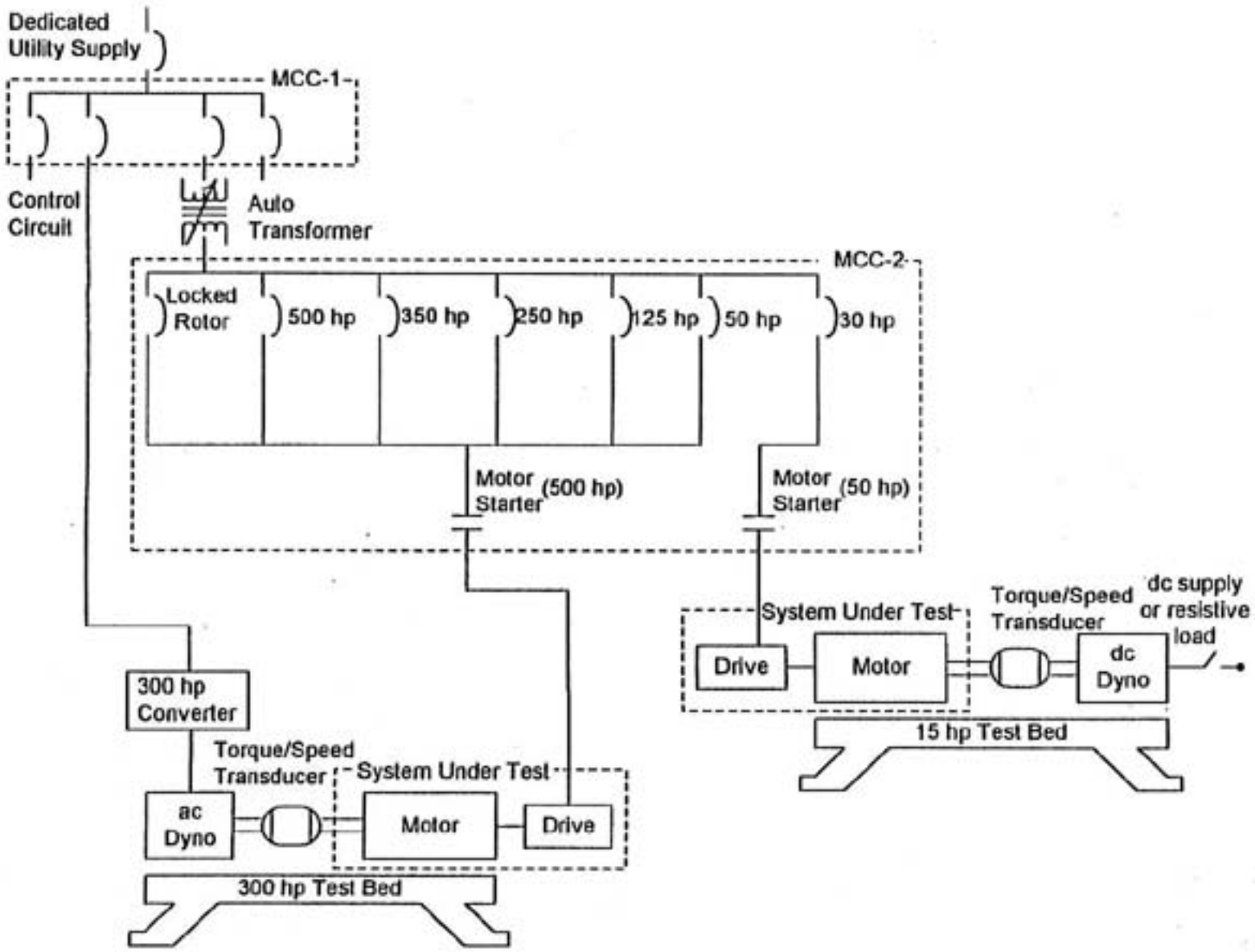

Fig. 5 Schematic of MSRF Test Laboratory

The electrical input to the three systems under test, motor alone, motor powered by a VFD, and motor driving via an ASCS, was measured by a Voltech, model PM3300, power analyzer. Three phase current signals for the power analyzer were obtained by LEM transducers. Specifications of the PM3300 are given in Section 9.A.3: the frequency ranges being significant for the input to the VFD power systems in particular. The PM3300 enables measurements of true rms quantities, fundamental and major harmonic components and total harmonic distortion factors (THD). The Voltech/LEM system has been end-to-end calibrated using a Fluke model MC5500A multicalibrator.

The isometric diagram of Fig. 6 depicts the conventional configuration of the 300hp test bed. For this study the configuration was modified by the introduction of an additional shaft, supported by pillar-block bearings, to protect the torque transducer bearing from any transverse loads that might be generated in the tests. In addition mechanical support was provided for the ASCS clearance adjustment mechanism. Fig. 7a shows the complete test bed arrangement and Fig. 7b shows the 200hp ASCS, adjusted to maximum clearance (lowest speed) during the test program.

3. Baseline Systems

In order to provide a basis for justifiable comparisons of throttled systems with both ASCS and VFD controlled systems, investigations of the performance of both a fan and a pump were made to establish baseline characteristics. These test characteristics were then scaled to the 50hp, 100hp and 200hp ratings of the ASCS and VFDs, and replicated with significant precision by the MSRF dynamometer.

3.1 Baffled Fan Tests

A large centrifugal fan, with flow-control baffles, 12ft. of ducting and an air-flow meter, was installed on the 300hp test bed in the position of the “client’s motor under test conditions” shown in Fig. 6. This enabled the fan to be driven under two different scenarios.

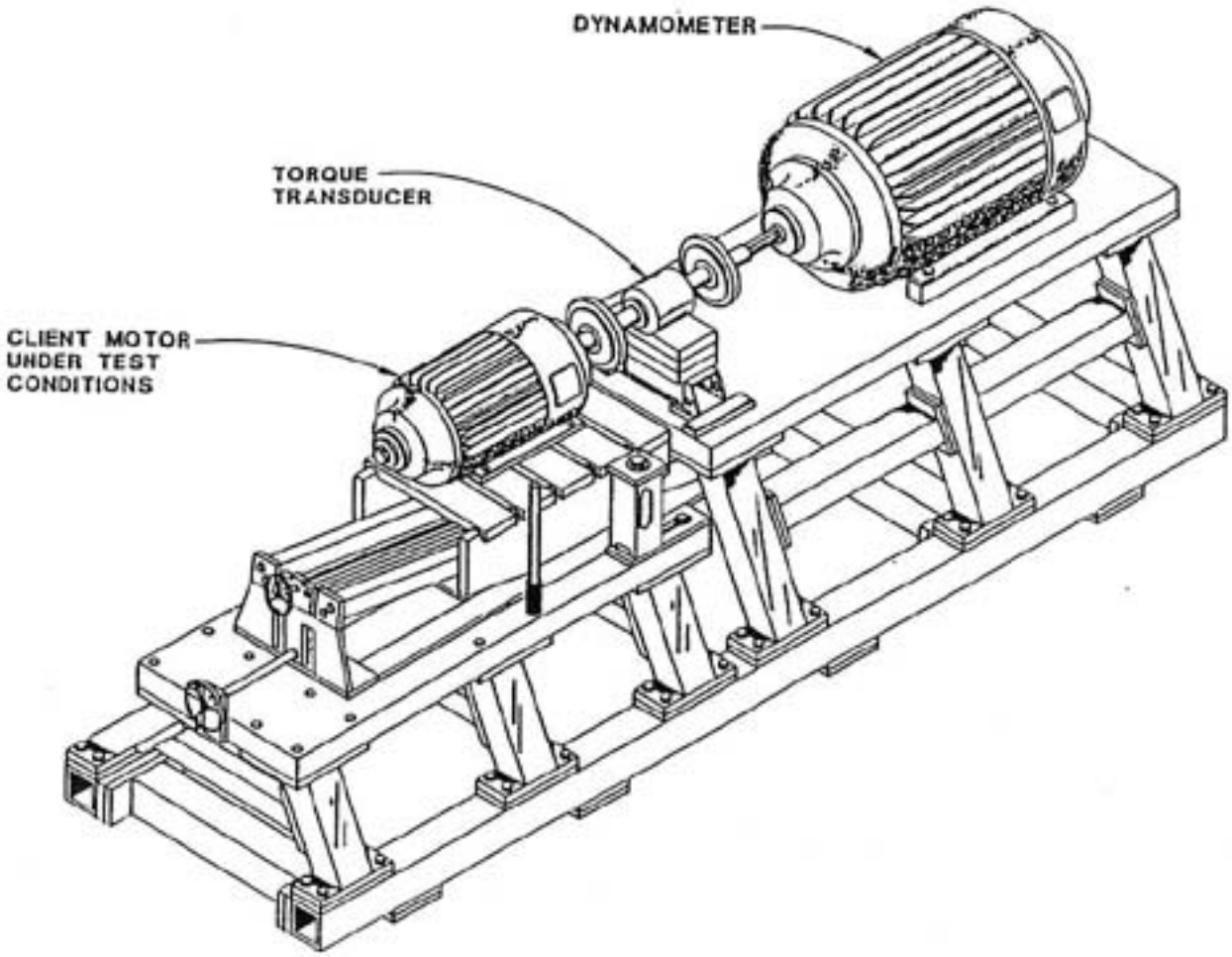

Fig. 6 Isometric Diagram of 300 hp Test Platform

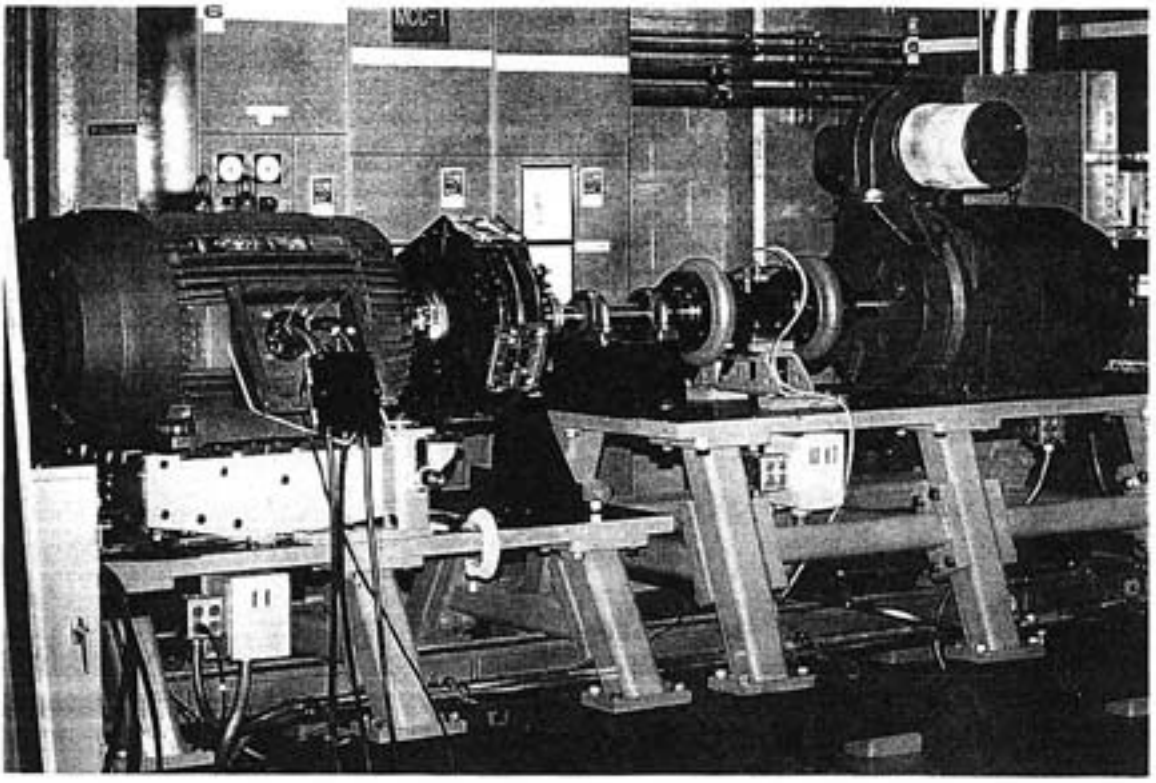

a

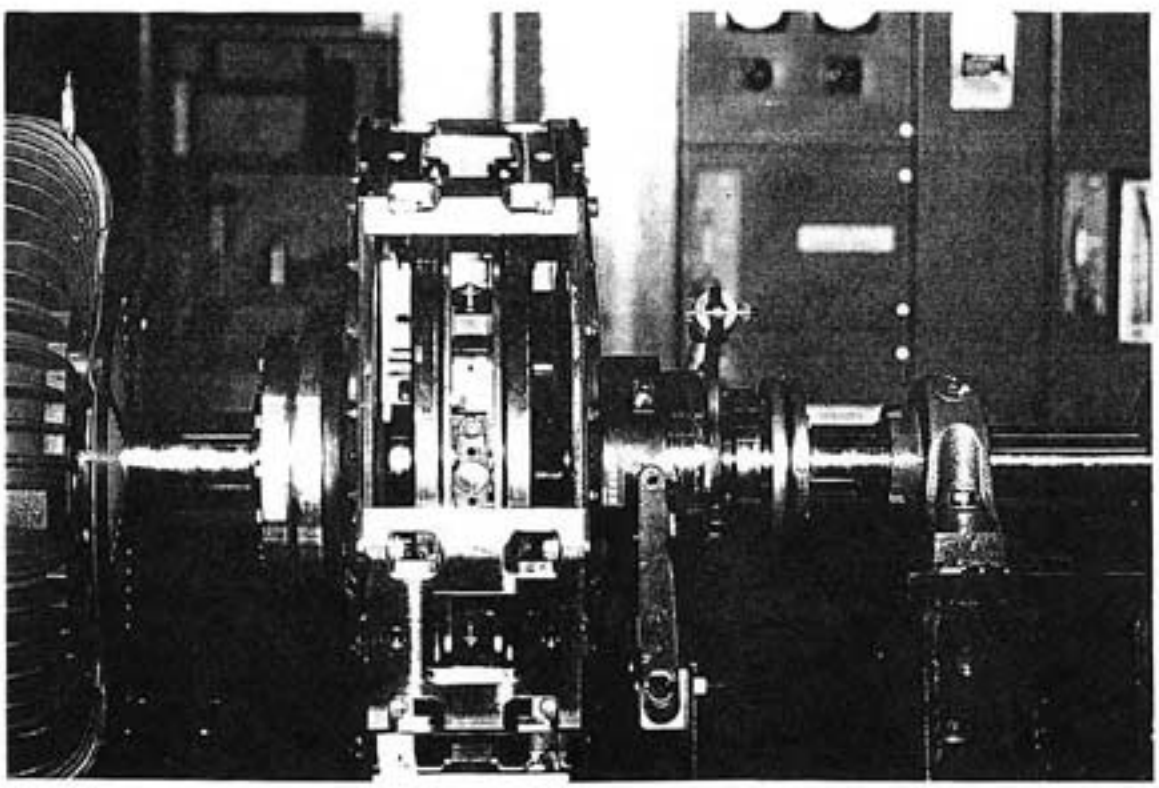

b

Fig. 7 Photographs of 200 hp ASCS Under Test

(i) The Fan was driven at a constant speed of 1800 RPM by the dynamometer, with the airflow controlled by baffles. The airflow was measured by an airflow meter for a range from 100% down to approximately 7% in 14 steps. The torque requirements for each flow setting were determined from the torque transducer on the input shaft of the fan.

(ii) The baffles were set wide open. The airflow was adjusted by changing the fan/dynamometer speed to match the 14-airflow setting achieved before. The torque requirements for each flow setting were determined as above.

To serve as a cross-check for errors or operational problems both tests (i) and (ii) were repeated and the data obtained is given in Appendix 9.B, sets 1 and 2. From the torque and speed of the input shaft of the fan the input power requirements were calculated. The results are shown in Fig. 8.

3.2 Throttled Pump Tests

MagnaDrive Corp. has constructed a traveling demonstration of a 15 hp pump system on a flatbed truck. The demonstration system can be operated in a throttling mode, with the ASCS coupling set at minimum slip and a valve used to control flow; or in a speed control mode, with the throttling valve set wide open and the ASCS controlling the speed and flow of the pump. Measurements were made on this system when it visited the OSU MSRF for a demonstration. The results are tabulated in Appendix 9.B, Set 3 and are presented graphically in Fig. 9.

3.3 Scaling for Rated Horsepower

The fan and pump data obtained from the tests described in Sections 3.1 and 3.2 does not correspond directly to the three ratings (50hp, 100hp, and 200hp) of the ASCSs and VFDs to be evaluated. Consequently this data was scaled to the required torque vs. flow characteristics which have the required peak levels. These scaled requirements are shown in Figs. 10(a) and 10(b), for fans and pumps respectively and were used to set the operating conditions of the dynamometer in the tests described in the next two sections of this report.

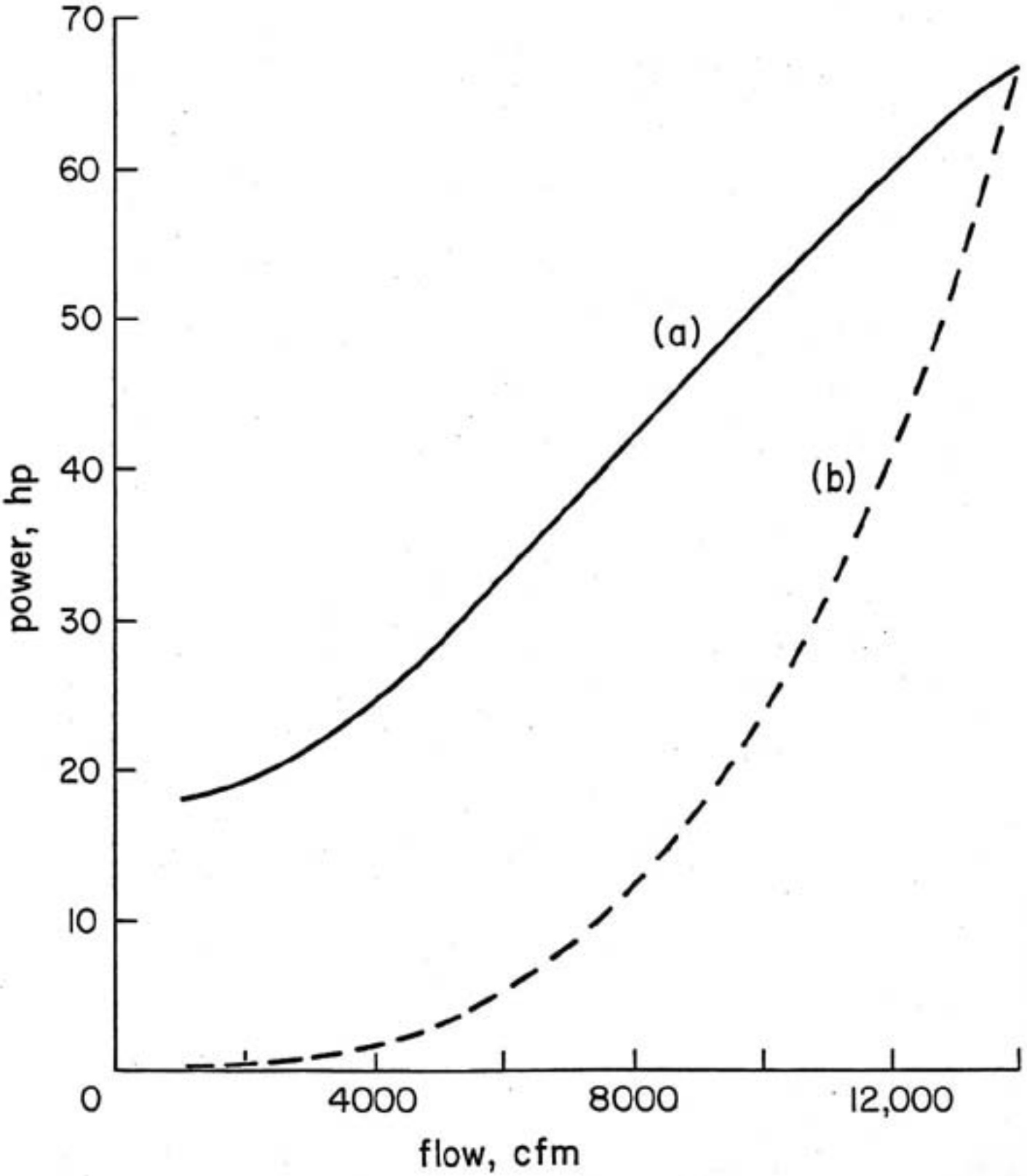

Fig. 8 Baseline Data for "100 hp" Fan Operation
a) Flow Controlled by Baffling
b) Flow Controlled by Fan Speed Adjustment

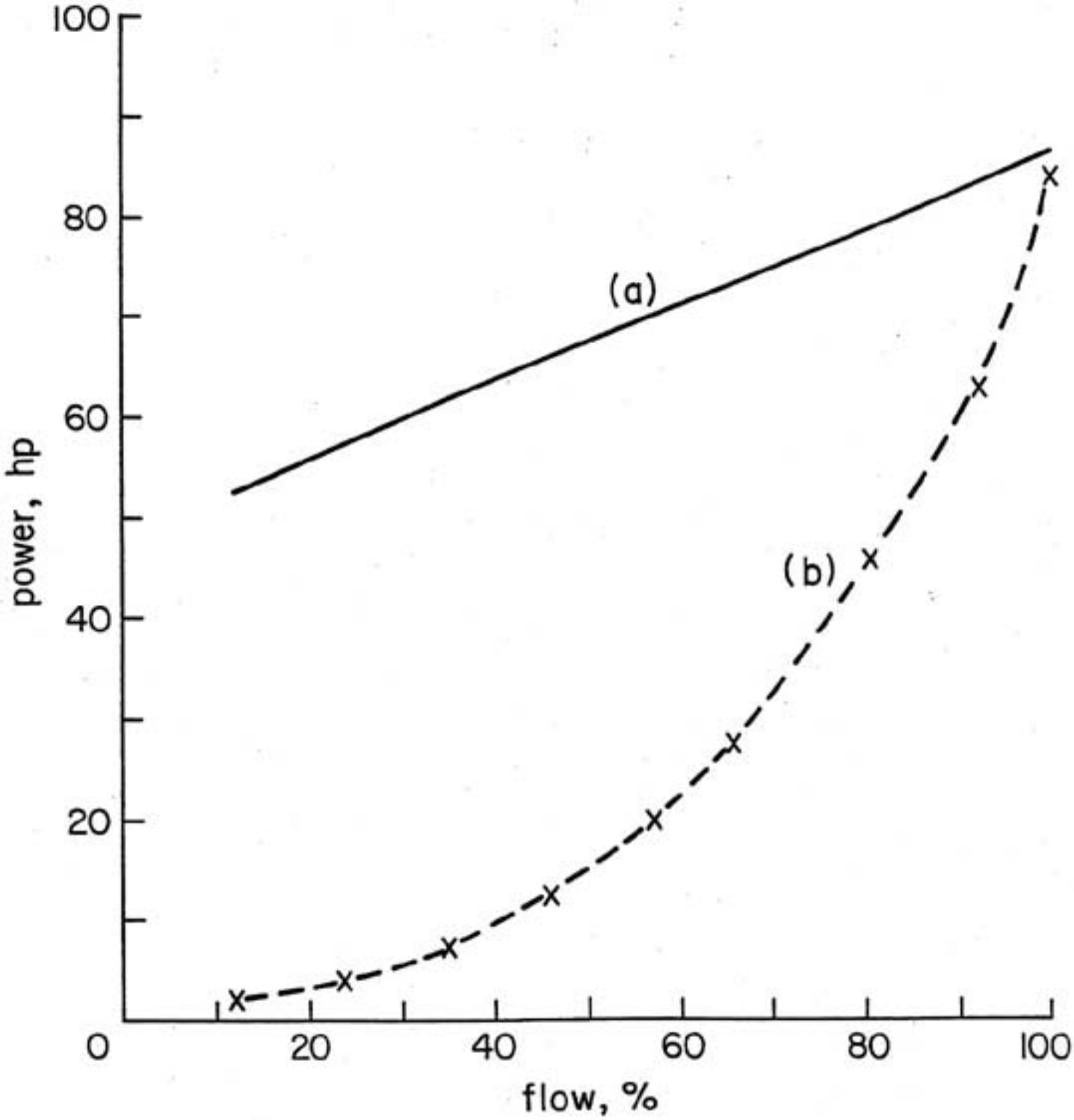

Fig. 9 Baseline Data for "100 hp" Pump Operation
a) Flow Controlled by Throttling
b) Flow Controlled by Pump Speed Adjustment

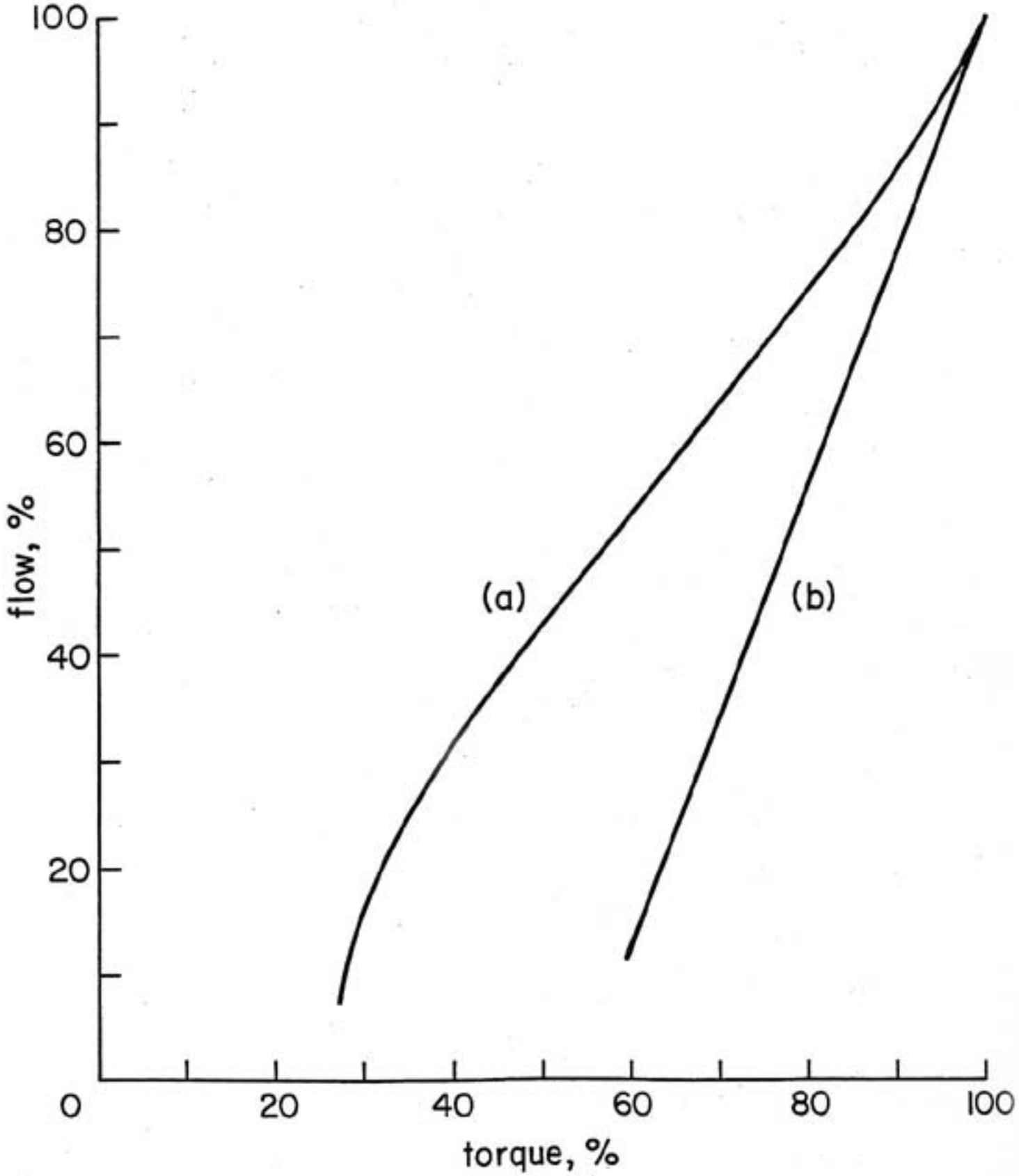

Fig. 10 Scaled Torque Requirements for Given Flow Rates
a) Fans
b) Pumps

4. Test Results for Adjustable-Speed Coupling System (ASCS)

Each of the three ASCSs tested was mounted in the test stand, between the appropriately rated induction motors and the torque/speed transducer, as shown in Fig. 7. Two of these ASCS units, the 50hp and the 200 hp are shown in Fig. 11 after use in the test program. The induction motors were connected directly to the laboratory 460V service which is maintained at rated value and fully balanced by the autotransformers shown in Fig. 5.

From the baseline tests described in the previous section the torque-speed requirements given in Tables 1 and 2 for the direct coupled/throttled systems, and Tables 3 and 4 for the adjustable speed systems, were developed. These performance points are required for the dynamometer to simulate both throttled (and baffled) and adjustable speed operation, and were set as follows. First the exact required operating speed was set by the MSRF dynamometer (now acting as a load). The torque corresponding to the required speed was then set by adjustment of the clearance of the ASCS. The multiple-turn adjustment mechanism used to set the clearance enabled very precise replication of the required points, as is evident throughout the test data given in Appendix 9.B. Having established a specific speed and torque condition, the system was left to operate in steady-state condition until all performance variables (particularly temperature) had stabilized. The following parameters of operation were then recorded:

(a) speed and torque (required values);
(b) electrical input voltage, current, power, true power factor (including harmonic distortion components), and total harmonic distortion (THD) of both voltage and current;
(c) sound levels at 20 ft from the test bed;
(d) vibrations, as the horizontal vertical and axial acceleration, at the drive motor bearing;

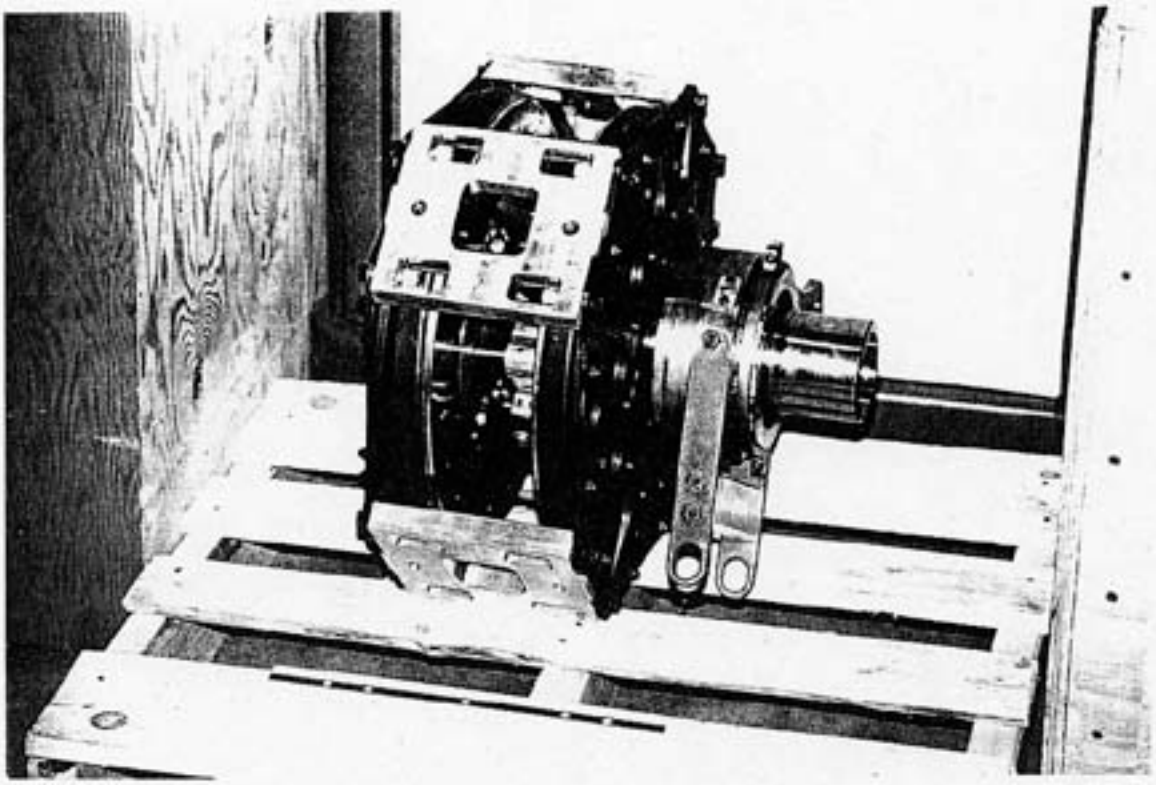

a

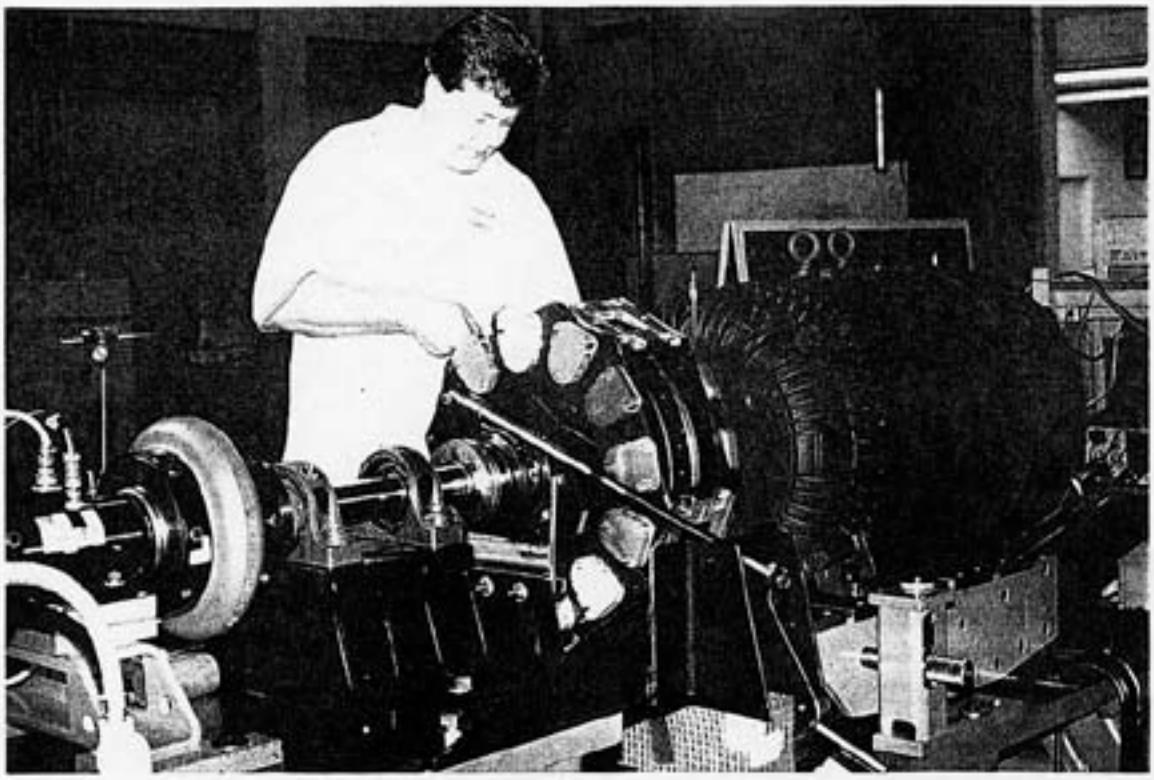

(b)

Fig. 11 Photographs of ASCS Equipment
a) 50 hp ASCS After Testing
b) 200 hp ASCS During Installation

(e) ambient temperature and the temperatures at the ASCS collar, both magnet discs and both conductor discs, plus motor bearing temperature.

To serve as a cross-check for errors or operational problems all the tests were repeated. Consequently, with the exception of the VFD tests for 200hp, two data sets are given in Appendix 9.B for each of the tests. Comparison of these shows that a high degree of repeatability was achieved.

Table 1 – Torque Targets (N) for Fan Simulation
Direct Coupled (1785-1800 r/min) and Baffled

Flow Rate %	100	93	86	79	71	64	57	50	43	36	29	21	14	7
50hp Motors	198	190	177	166	153	139	125	113	99	86	74	64	59	53
100hp Motors	396	380	354	331	306	278	250	225	198	172	149	128	117	107
200hp Motor	792	759	708	663	612	556	501	450	396	343	297	256	235	214

Table 2 – Torque Targets (N) for Pump Simulation
Direct Coupled (1785-1800 r/min) and Throttled

Flow Rate %	100	92	81	69	58	46	35	23	12
50hp Motors	201	194	183	172	162	152	141	130	119
100hp Motors	402	388	366	345	324	303	282	260	238
200hp Motor	804	776	732	690	648	606	564	520	476

Table 3– Torque Targets (N) for Fan Simulation
Adjustable Speed Operation

Flow Rate %	100	93	86	79	71	64	57	50	43	36	29	21	14	7
Target Speed r/min	1800	1659	1530	1400	1270	1150	1020	890	759	629	490	370	310	230
50hp Motors	198	169	144	123	99	82	66	50	37	26	16	10	7	5
100hp Motors	402	343	292	250	201	166	133	102	74	52	33	20	15	10
200hp Motor	792	675	574	493	396	327	262	201	147	103	65	39	30	19

Table 4– Torque Targets (N) for Pump Simulation

Adjustable Speed Operation

Flow Rate %	100	92	81	69	58	46	35	23	12
Target Speed r/min	1698	1531	1363	1173	990	803	608	429	284
50hp Motors	201	168	138	108	84	64	48	36	29
100hp Motors	402	336	275	216	167	128	97	73	58
200hp Motor	804	671	550	432	334	256	194	146	116

4.1 New 50hp Motor

A brand new 50hp, NEMA 841 standard, 4-pole induction motor from a major manufacturer was used throughout these tests. The data sets for baffled fan and throttled pump operation are given in Appendix 9.B – Set 4 (a) and (b). The corresponding data sets for ASCS control are given in Appendix 9.B – Sets 5(a).1 and 5(a).2, and Sets 5(b).1 and 5(b).2. The following observations are made from the direct comparison of data Sets 4 and 5.

4.1.1 Speed and Torque

The measured (test) torque conditions met the required values to a highly acceptable level. Under ASCS operation the motor speed increased more than under throttling or baffling operation due to the substantial off-loading experienced as the slip of the ASCS increased.

4.1.2 Electrical Power Input and Utilization

The operational efficiency of the motor remains high as a function of load flow for throttled and baffled operation, whereas the efficiency of the motor and ASCS falls off rapidly with decreasing load. This direct comparison is misleading, however, as throttling and baffling waste significant energy in the valves and baffles themselves. More meaningful comparisons are the power input as a function of flow, indicating overall system process efficiency. These are shown in Figs. 12 and 13, where substantial savings for ASCS operation are demonstrated.

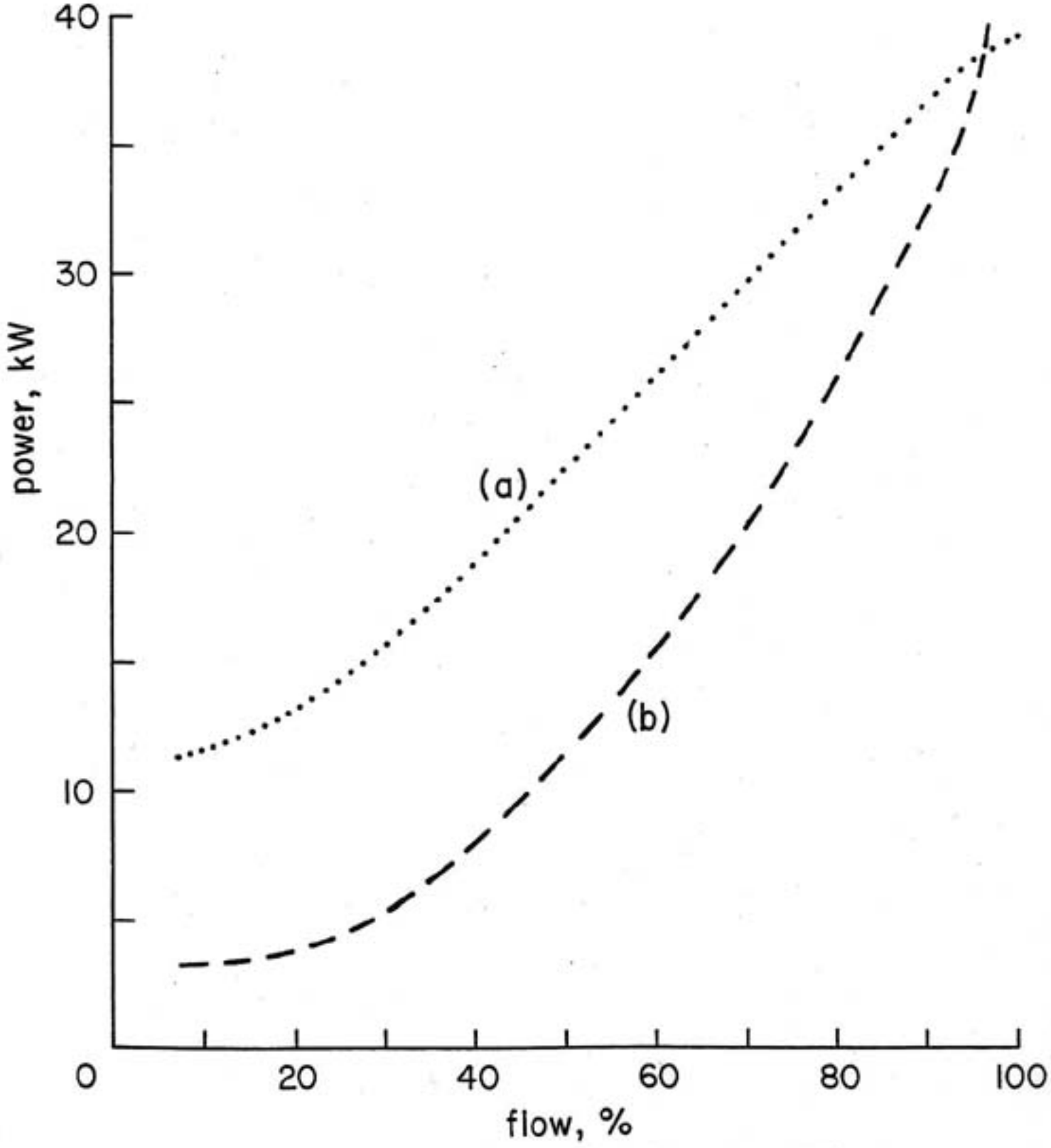

Fig. 12 Input Power for Flow Requirements for Fan Driven by New 50 hp Motor
a) Direct Drive and Output Baffles
b) Drive Via ASCS

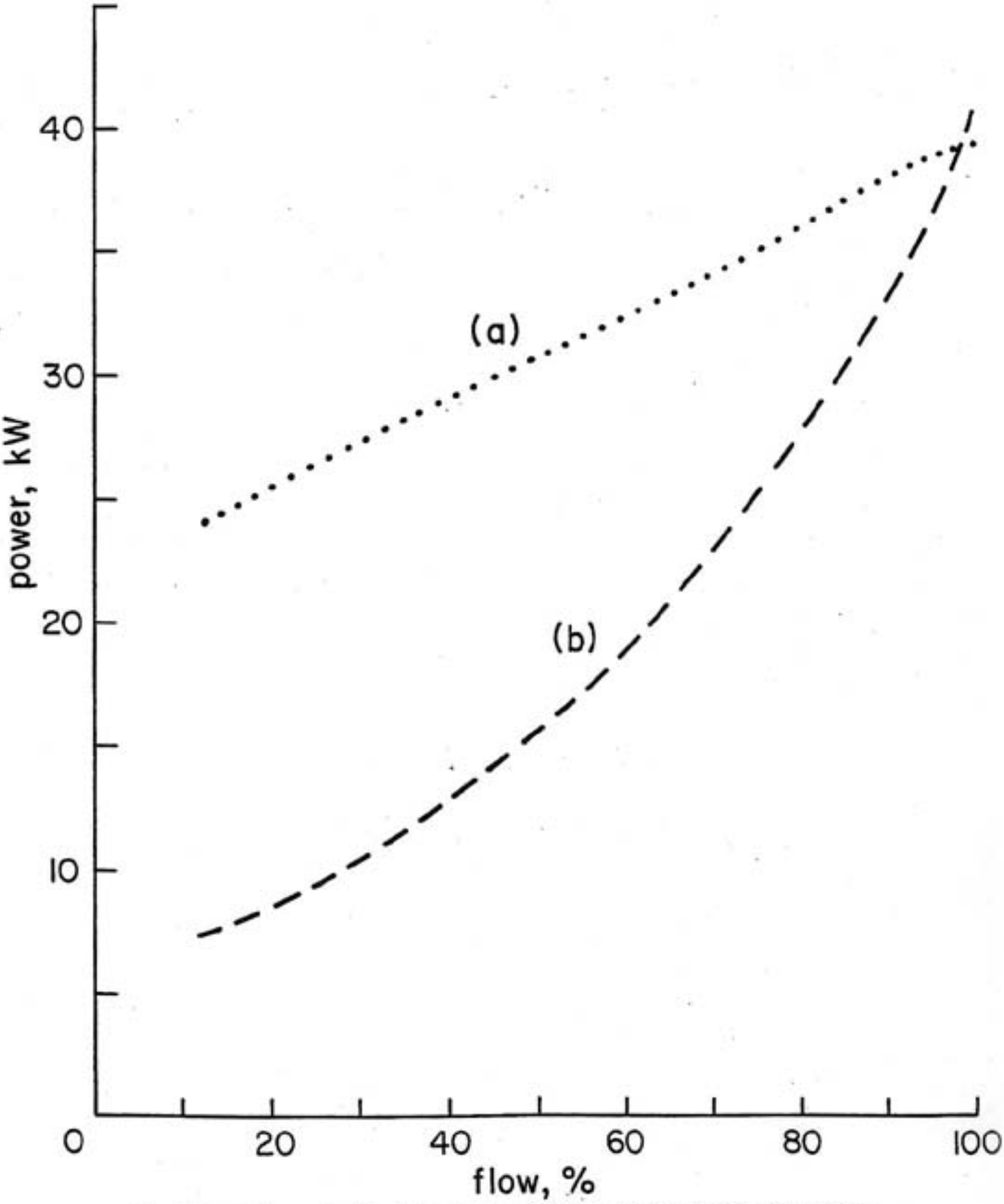

Fig. 13 Input Power for Flow Requirements for Pump Driven by New 50hp Motor
a) Direct Drive and Output Throttle Valve
b) Drive Via ASCS

4.1.3 Power Factor and Total Harmonic Distortion

Power factor of the motor is shown to reduce more with ASCS operation than with throttling. This is to be expected as the ASCS causes the motor to be off-loaded far more. This need not be a problem as correction techniques for power factor are widely employed in industry. The power factor for the ASCS fan simulation is higher that the VFD system for all flows from 100% to 50% of maximum flow. The power factor for the ASCS pump simulation is higher than the VFD system for all flows from 100% to 12% of full flow.

The THD of input currents of the ASCS and the throttled systems are essentially similar, at 3% voltage distortion, and 5-10% amp distortion. This is similar to the 3% voltage distortion of the VFD system, but is substantially less than the 105-215% amp distortion for the VFD system.

4.1.4 Sound Levels

Sound levels for the 50 hp ASCS were consistently approximately 80 db. This compares to 74 to 80 db for the throttled fan and throttled pump simulations. The increase in db is attributed to windage from the unshrouded ASCS coupling.

4.1.5 Vibration

No balancing or precision alignment was performed on the ASCS installation. The vibration levels for all installations were similar, ranging from 0.007 to 0.058 ips. The levels measured were not a cause for concern.

4.1.6 Motor Bearing Temperatures

As is shown in Figs. 14 and 15, for both fan and pump loads the motor bearing temperature for throttled operation changes very little as a function of load. With the ASCS, however, the motor bearing temperature reduces as the load decreases.

4.1.7 ASCS Temperatures

Monitoring of the temperatures of the magnet discs and the conductor discs of the ASCS presents some difficulties of consistency: these are complex and composite structures rotating at significant speeds. A hand-held, laser-

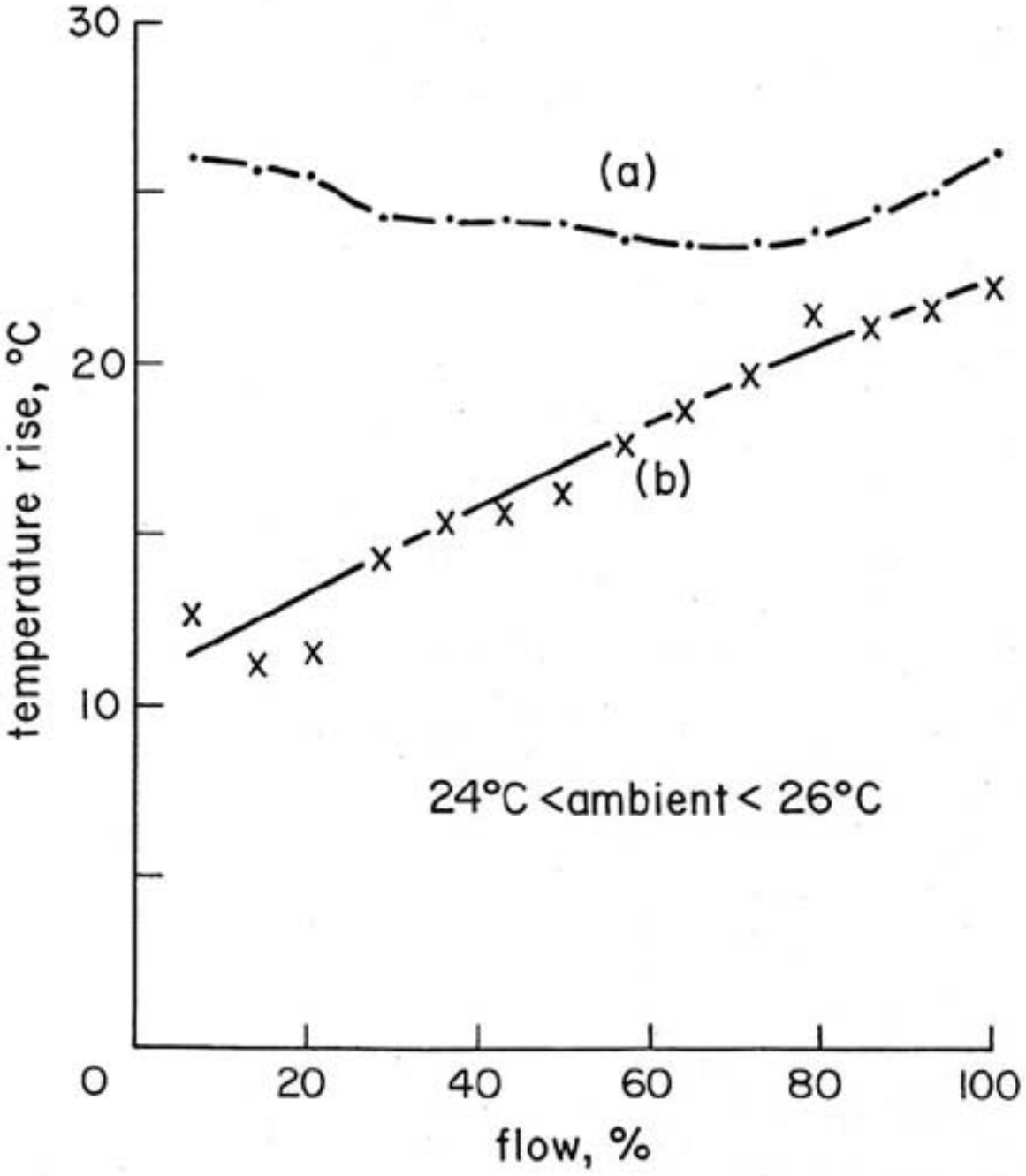

Fig. 14 Temperature Rise of Shaft-End Bearing of New 50 hp Motor Driving Fan Load
a) Flow control by Baffles
b) Flow Control by ASCS

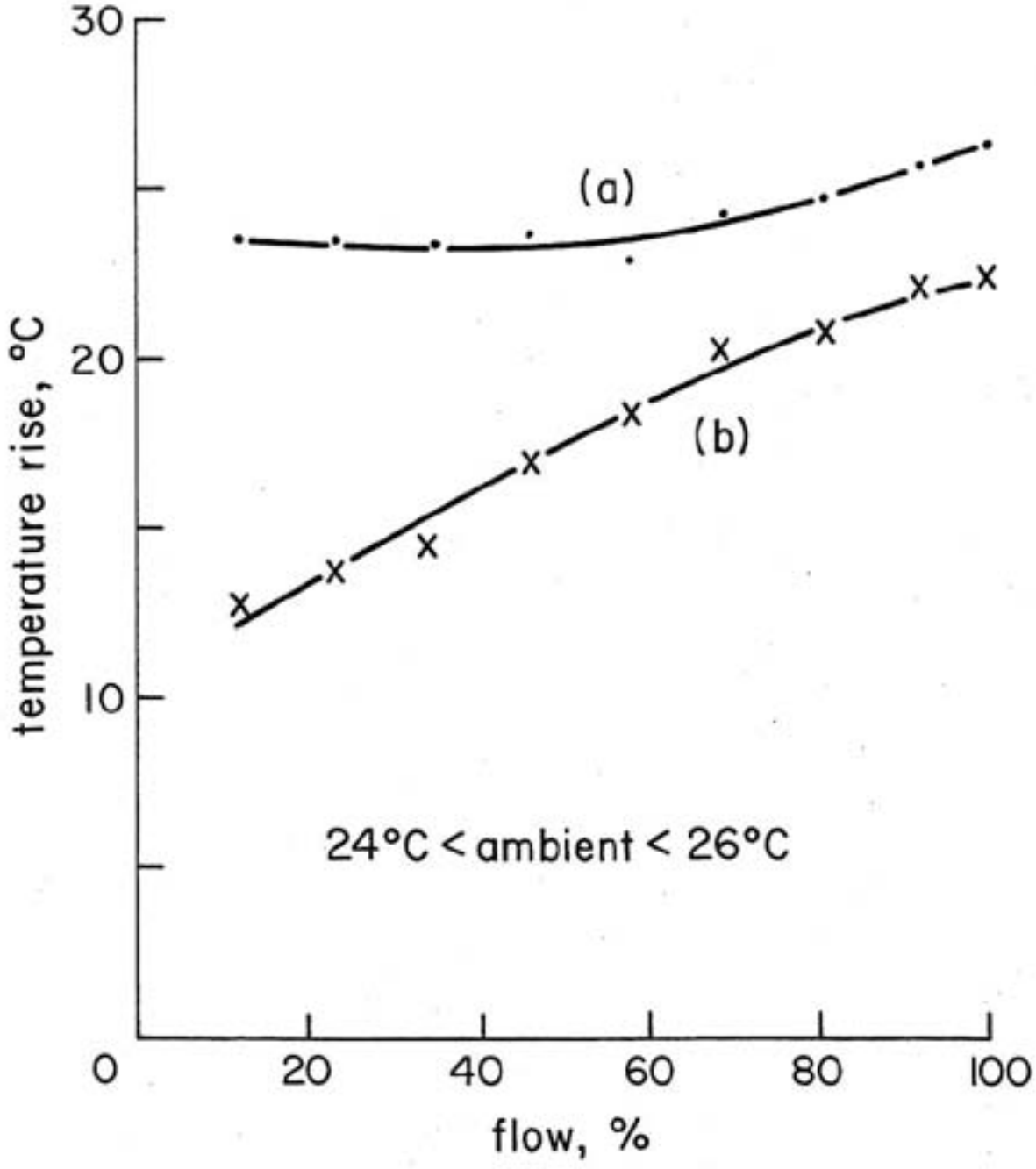

Fig. 15 Temperature Rise of Shaft-End Bearing of New 50 hp Motor Driving Pump Load
a) Flow Control by Throttle Valve
b) Flow Control by ASCS

pointed, temperature indicator was employed to provide the measurements and the ambient was provided by the Fluke Multicalibrator. The resulting temperature rise data is given in Figs. 16 and 17. The scatter of the test points indicates the difficulty encountered in these measurements, however the general trends are evident. For fan operation the conductor discs had a maximum temperature rise between 70°C and 80°C, and the magnet discs rose 20°C to 30°C, above ambient. Because of the static head, the pump duty is more onerous and consequently the temperature rises shown in Fig. 17 are a little higher than those given in Fig. 16 for the fan operation. None of these indicate any problem for the materials involved. In particular the curie temperature of the magnet material (≈ 150°C) was never threatened. The 50 hp ASCS coupling does not require cooling fins, which are provided on some of the larger ASCS configurations.

4.2 Old 50hp Motor

In order to provide an assessment of the viability of the use of the ASCS with motors other than new, high efficiency models, the set of tests described in Section 4.1 was repeated using an old, repaired, 50hp 4-pole motor which was purchased for this study from a stock of refurbished machines. The data sets for baffled fan and throttled pump operation are given in Appendix 9.B – Set 6 (a) and (b). The corresponding data Sets for ASCS control are given in Appendix B – Sets 7(a).1 and 7(b).2. The following observations are made from the direct comparisons of data Sets 6 and 7, and also with Sets 4 and 5.

4.2.1 Speed and Torque

As for the new 50hp motor, it is evident that the measured torque levels set during the tests met the target values to an acceptable degree: generally to better than 1%. Comparison of the throttled and baffled characteristics of the two 50hp motors gives the surprising result that, for a given required torque the old motor operated at a higher speed than the new motor. At the highest load conditions this difference was in the range of 5 to 6 rev/min, reducing to 2 to 3 rev/min at the lowest loads. For ASCS testing the speeds of the two motors were

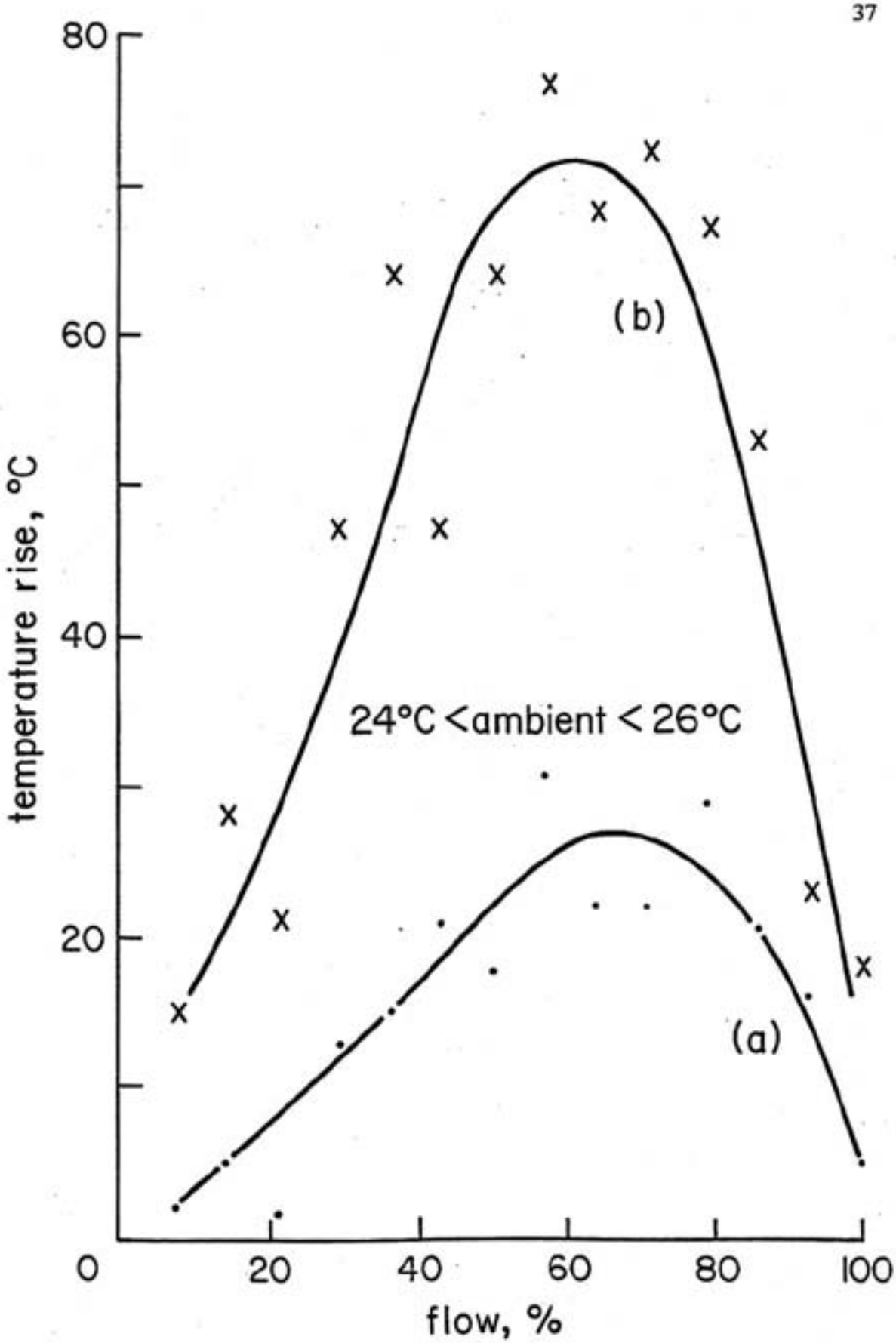

Fig. 16 Temperature Rise of ASCS Discs Providing Fan Load from New 50 hp Motor
a) Magnet Disc Temperature Rise Above Ambient
b) Conductor Disk Temperature Rise Above Ambient

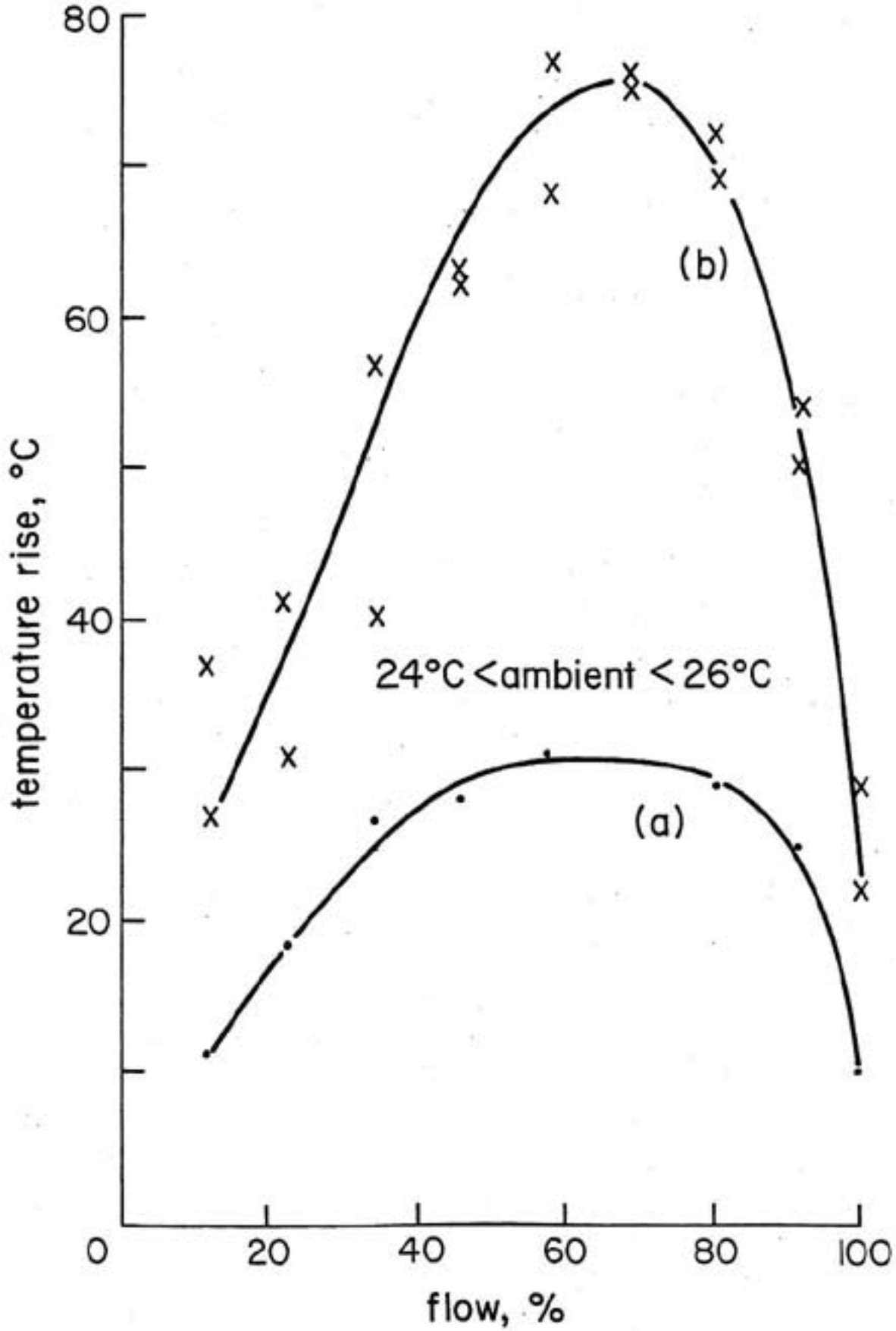

Fig. 17 Temperature Rise of ASCS Discs Providing Pump Load from New 50 hp Motor
a) Magnet Disc Temperature Rise Above Ambient
b) Conductor Disk Temperature Rise Above Ambient

effectively dictated by the programming of the dynamometer. Consequently the speeds corresponded to within 1 rev/min.

4.2.2 Electrical Power Input and Utilization

The efficiency of the old motor, when driving the throttled and baffled loads was always lower than that of the new motor under corresponding conditions. The differences range from approximately 2 percentage points at the higher loads, increasing to approximately 7 percentage points at the lowest loads for the fan characteristic. Otherwise the trends and differences of the direct coupled and the ASCS coupled were comparable to the corresponding test results for the new 50hp motor. The comparisons of input power as functions of flow are given in Figs. 18 and 19.

4.2.3 Power Factor and THD

The overall trends of power factor and THD as a function of flow rate for both ASCS and throttling operation were very similar for the old 50hp as for the new 50hp discussed in Section 4.1.3. A comparison of the levels of power factors show that, for a given operating point, the old 50hp motor has slightly better power factor than did the new 50hp motor. This is indicative of higher losses in the older, repaired, machine. Total harmonic distortion levels are almost identical for the two motors and is not a cause for concern.

4.2.4 Sound Levels

The sound levels observed for ASCS control of flow are typically 1 to 2 dB higher than the corresponding level for throttling. Related to an 80 dB base this is not significant and is probably due to the windage of the ASCS itself. The sound levels produced using the old 50hp motor are generally 2 to 3 dB higher than the corresponding values for the new 50hp motor.

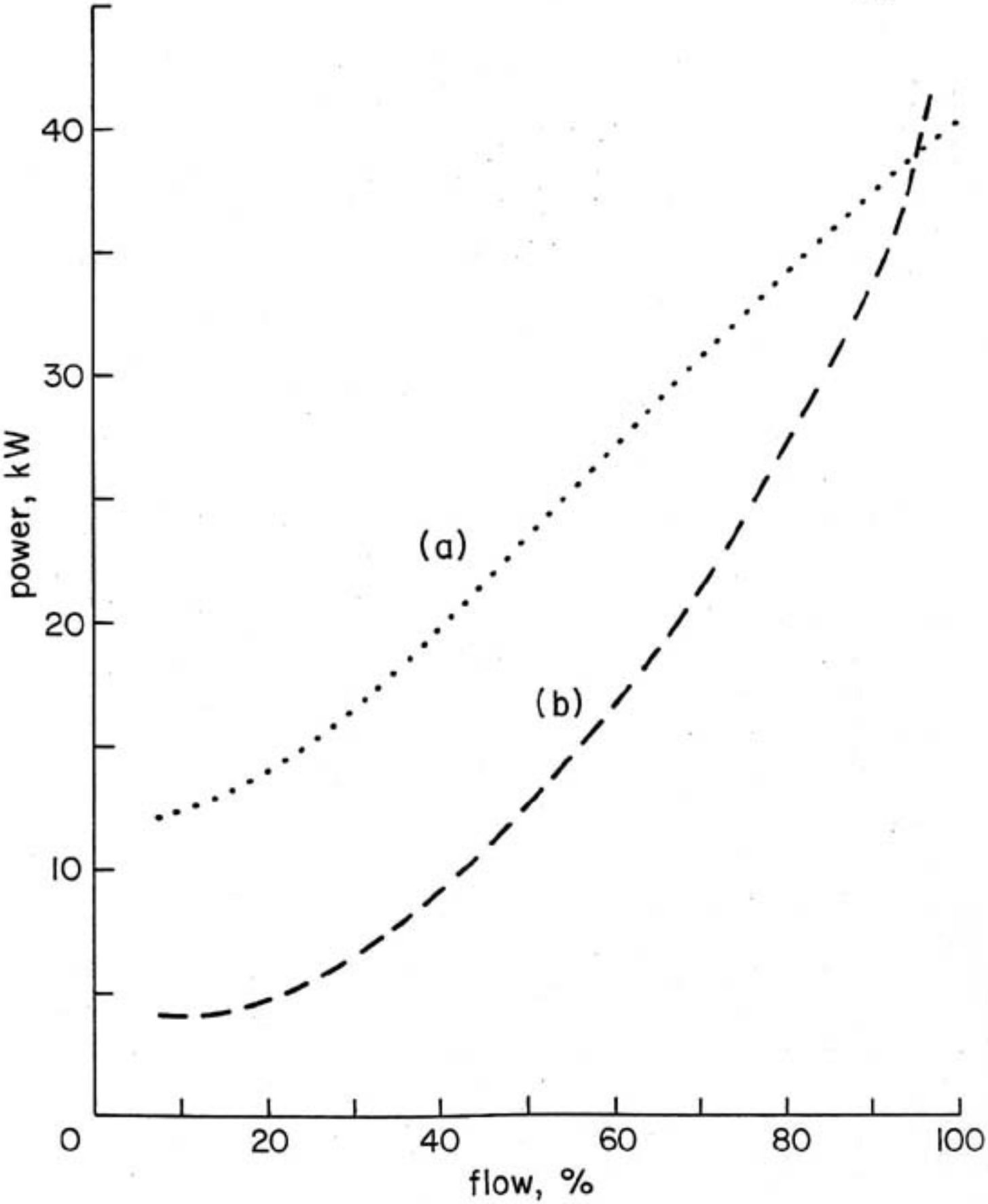

Fig. 18 Input Power for Flow Requirements for Fan Driven by Old 50 hp Motor
a) Direct Drive and Output Baffles
b) Drive Via ASCS

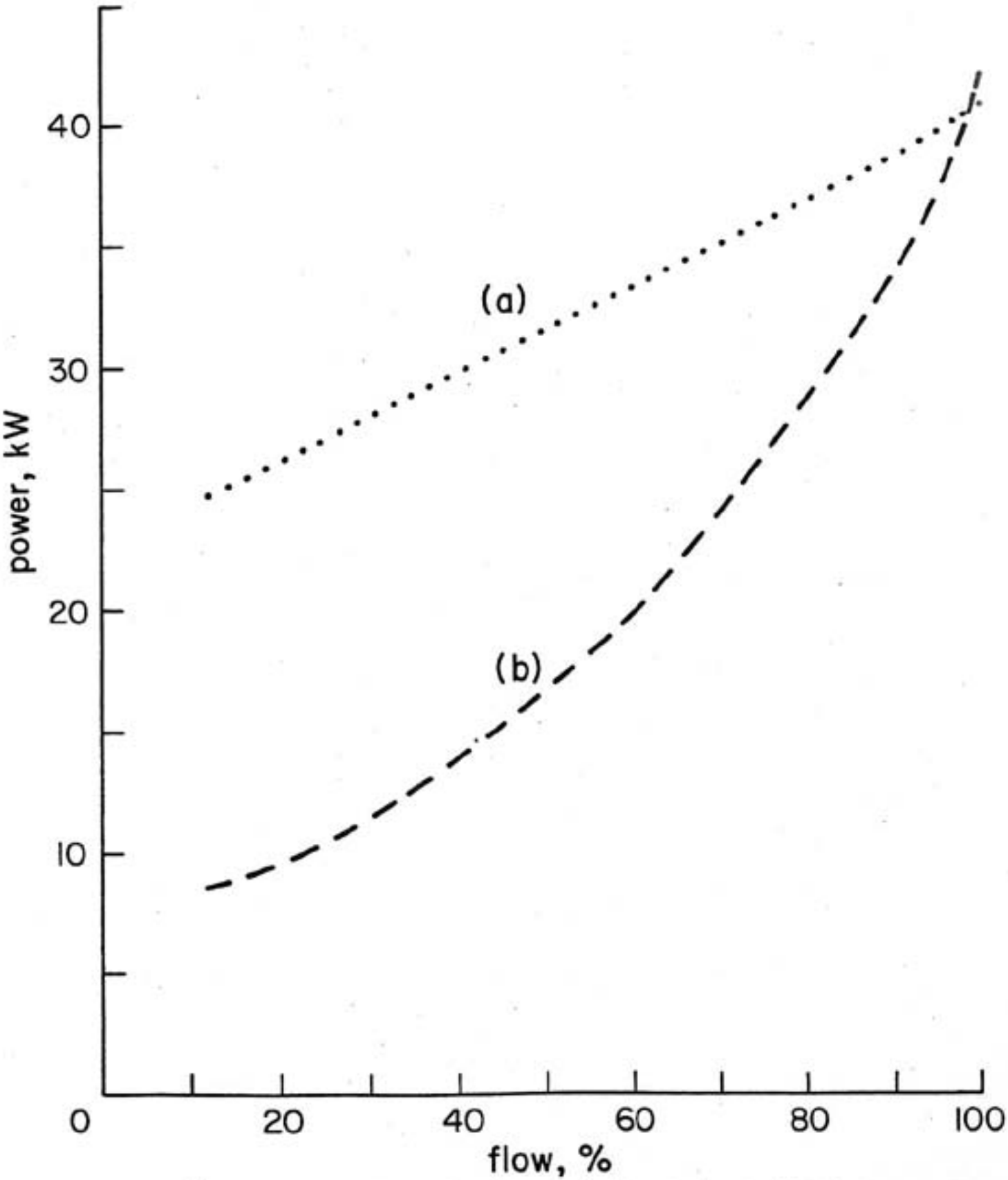

Fig. 19 Input Power for Flow Requirements for Pump Driven by Old 50 hp Motor
a) Direct Drive and Output Throttle Valve
b) Drive Via ASCS

4.2.5 Vibration

Overall the recorded vibration levels are slightly lower using the ASCS than when connected via the Omega coupling. The levels are not of any particular consequence.

No particular trends are evident in vibration level comparisons between the old 50 hp and the new 50 hp motors.

4.2.6 Motor Bearing Temperatures

It is evident from the data presented in Figs. 20 and 21 that the motor bearings operate in the range of 6 to 8°C higher when driving the loads via the ASCS. However at light loads this difference reduces to zero.

Compared to its new 50hp counterpart, the old 50hp motor generally operated with bearing temperatures at least 20°C lower, as seen by comparisons of Figs. 20 and 21 with Figs. 14 and 15. This is probably due to the tightness of the new bearings which may require many hours of operation before they are truly 'broken-in'. Overall, the use of ASCS at 50hp rating is not seen as having any detrimental effects on the motor or its bearings.

4.2.7 ASCS Temperatures

Figs. 22 and 23 show the temperature rise experienced in the discs of the ASCS 50hp coupling when driving fan and pump loads respectively. Again, considerable scatter of the test data points is observed representing, in part at least, the difficulty experienced in the taking of these measurements with the device in operation. In Figs. 22 and 23 two curves are given for the temperature rise of the magnet discs: these represent definite differences observed during the two runs of the test program. This lack of repeatability in the temperature rise of the magnet discs, which provided two very distinct curves for both load characteristics, is believed to be due in part to a looseness in the bearings of this older 50 hp motor which permitted significant axial movement of the rotor.

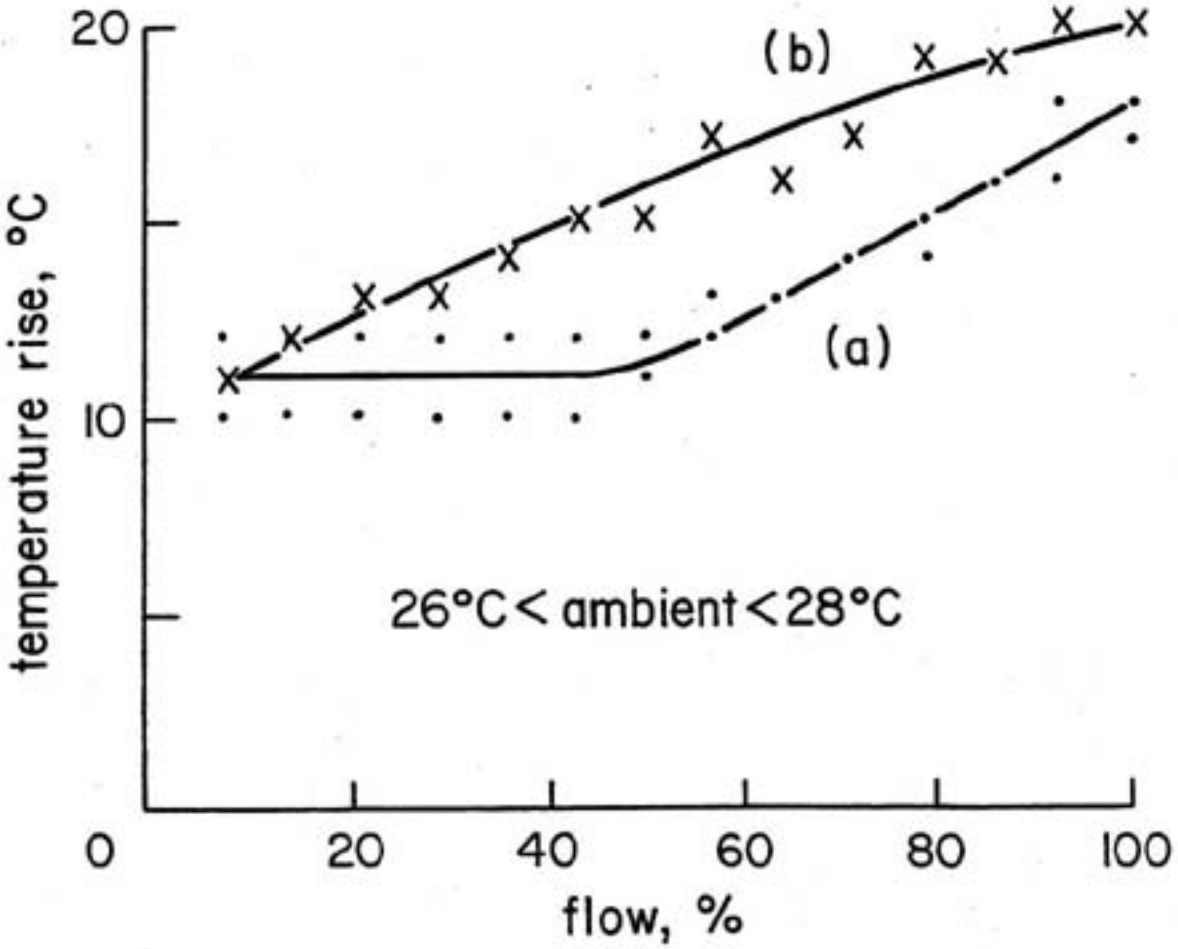

Fig. 20 Temperature Rise of Shaft-End Bearing of Old 50 hp Motor Driving Fan Load
a) Flow control by Baffles
b) Flow Control by ASCS

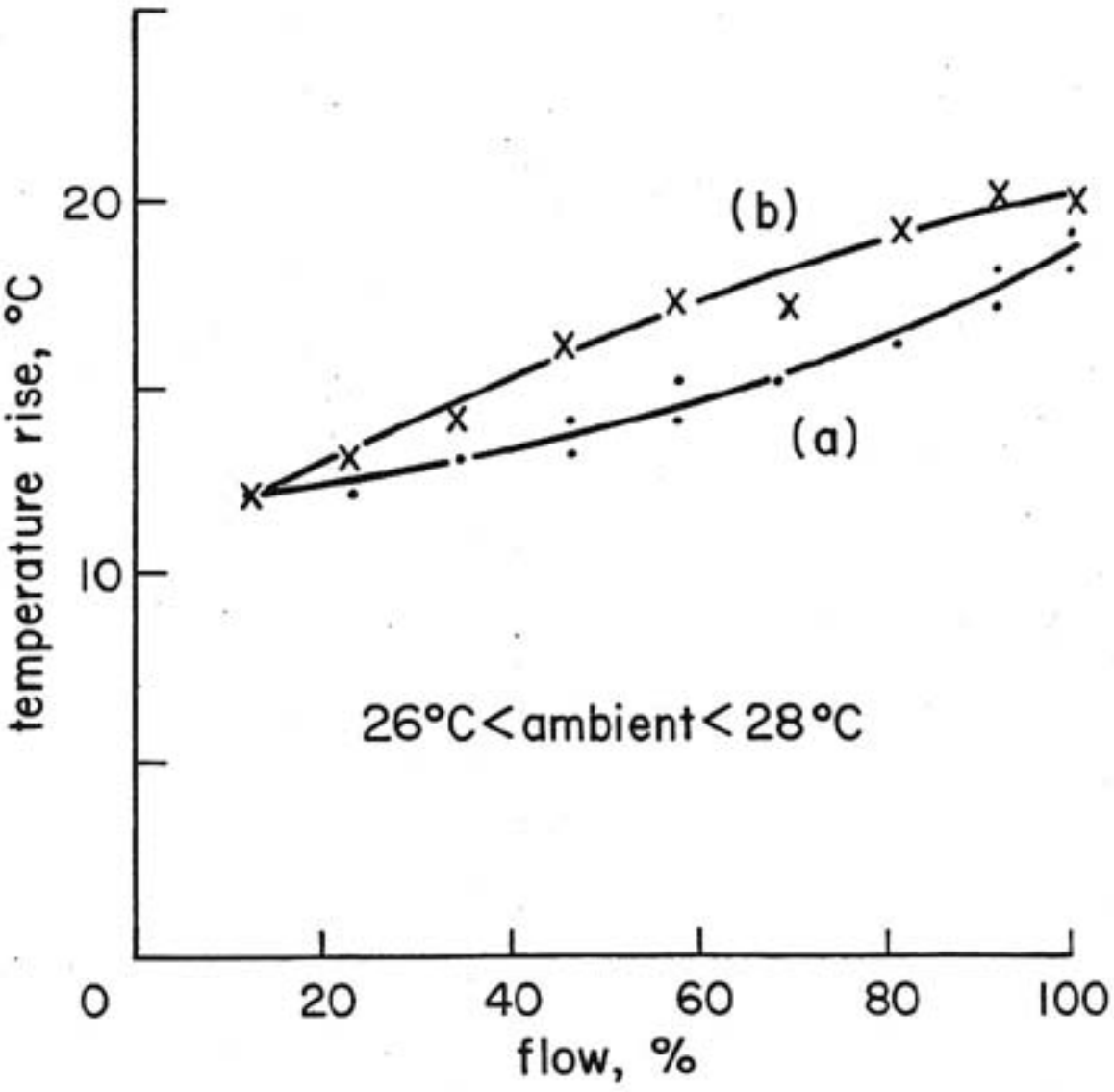

Fig. 21 Temperature Rise of Shaft-End Bearing of Old 50 hp Motor Driving Pump Load
a) Flow Control by Throttle Valve
b) Flow Control by ASCS

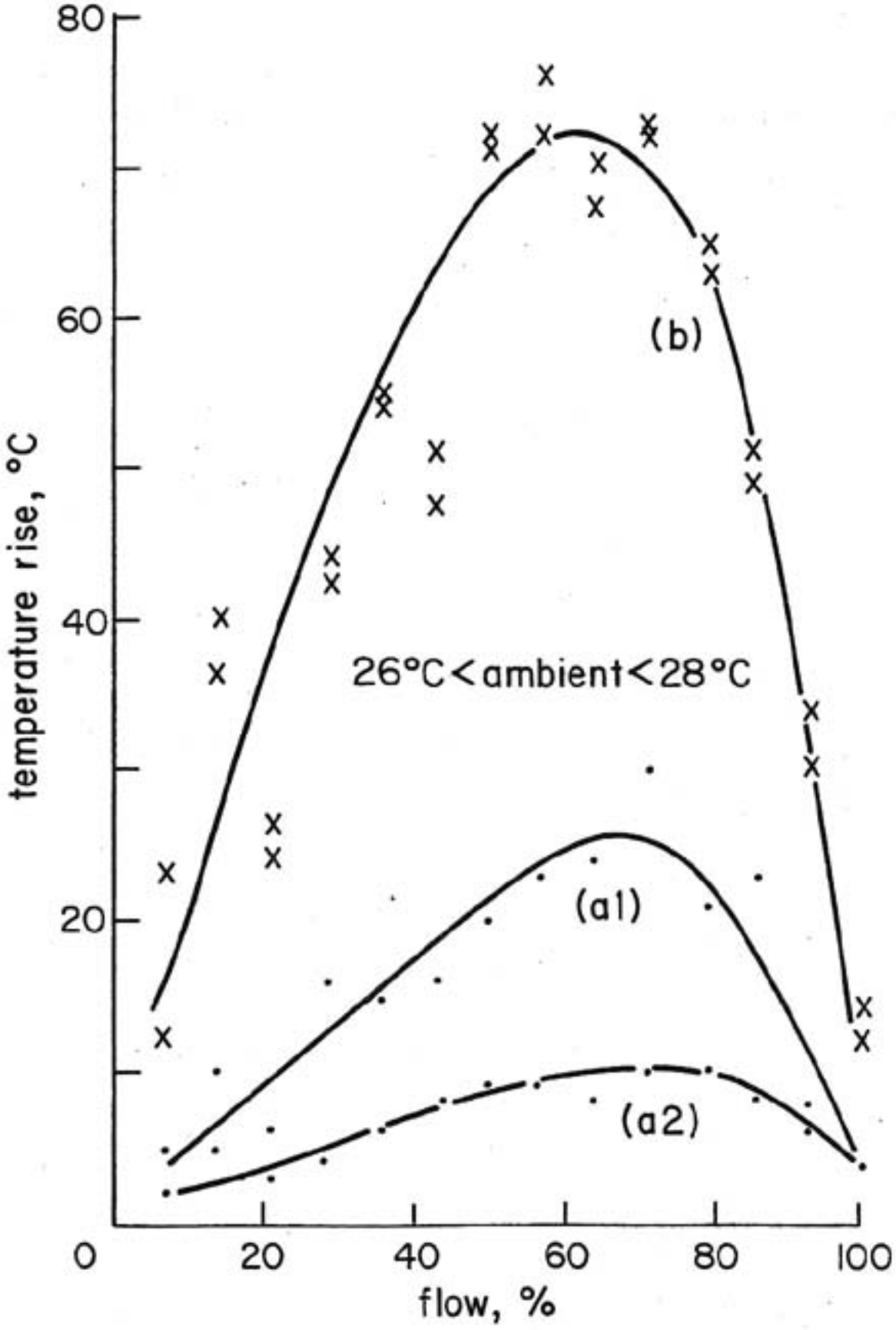

Fig. 22 Temperature Rise of ASCS Discs Providing Fan Load from Old 50 hp Motor
a) Magnet Disc Temperature Rise Above Ambient
b) Conductor Disk Temperature Rise Above Ambient

Hence the position of the ASCS discs could be different for the two test runs, although these were performed on the morning and afternoon of the same day.

Although the lack of repeatability of temperature rise in the discs is of concern the temperatures themselves are not. As expected the pump operation represents the more severe duty, but the approximately 30°C rise of the magnet discs and the 80°C rise of the conductor discs are well within safe margins for these materials.

There are no particularly marked performance differences between the temperature rises of the ASCS disc driven by the new 50 hp motor (Figs. 16 and 17) and when driven by the old 50 hp motor (Figs. 22 and 23).

4.3 New 100hp Motor

The motor used for the 100hp ASCS coupling tests was a brand new, NEMA 841, 4-pole induction motor from a major manufacturer. The data obtained from these tests are given in Appendix 9.B: Set 8(a) and (b)are for baffled fan and throttled pump operation; Set 9(a) and 9(b) cover the two tests for the fan and pump curves when ASCS was used. Chronologically these were the first tests performed on the ASCS in the MSRF and the data obtained, in consequence, reflect the inexperience and lack of test plan formulation of the test crew at the time. The test processes and recording techniques were still being developed as these tests proceeded.

The following observations are made from data Sets 8 and 9 and the corresponding graphs.

4.3.1 Speed and torque

The measured test values of torque, for the baffled and throttled tests, and of both torque and speed, for the ASCS controlled tests, are very close to the target values given in Tables 1 – 4. As observed for the 50hp tests, under ASCS operation the motor speed increases more than in the direct coupled tests as the load is reduced, indicating the substantial increase in off-loading that the ASCS enables.

4.3.2 Electrical Power Input and Utilization

As observed in the 50hp tests, reported in sections 4.1 and 4.2, the 100hp tests showed significant power reductions for ASCS control over baffled fans or throttled pumps. The power reductions are evident in Figs. 24 and 25 and the effects of ASCS are particularly beneficial for systems that operate at lower than maximum loads for substantial percentages of their operating times. Power reductions are greater for pump operation but, as will be seen in Figs. 28 and 29, the heating of the discs of the ASCS is greatest for pump operation (due to the static head component).

4.3.3 Power Factor and THD

The observations on power factor and total harmonic distortion presented in Sections 4.1.3 and 4.2.3 are equally valid here. The small differences in test data reflect primarily the differences in the motors rather than in the ASCS units.

4.3.4 Sound Levels

There is a significant measurable increase in the measured sound levels when the ASCS is used compared to the solid couplings. This increase is in the range of 10 to 12 dBA on a 77 to 78 dBA base. This is compared to the 2 to 3 dBA increase observed for the 50hp tests. The significant rise in the increased sound level is presumably due to the physical size of the ASCS units and the air disturbance resulting from their motion.

4.3.5 Vibration

No vibrational problems were observed in the tests and the recorded vibrational velocities are low.

4.3.6 Motor Bearing Temperatures

The general observation that the motor bearings appear to run hotter when driving a load via the ASCS rather than through a fixed coupling is valid from Figs. 26 and 27. These differences maximize at about 8 to 10 °C. However the trends of temperature rise shown in Figs. 26 and 27 do not show any particular correlation to the temperature rises of the other motors shown in Figs. 14 and 15, Figs. 20 and 21, and later in this report in Figs. 32 and 33. This lack of correlation is believed due to difficulties in the making and recording of these measurements and the relative inexperience of the test crew in working with ASCS equipment at the time of the 100hp unit tests.

4.3.7 ASCS Temperatures

The temperature rises above ambient of the ASCS discs are given in Figs. 28 and 29, for fan and pump duty respectively. As for the 50hp unit there is scatter of the test points about the estimated temperature rise characteristics. For the 100hp ASCS the magnet discs appeared to have a very similar temperature rise during the two tests of each load type. However, the temperature rise of the conductor discs differed when the tests were repeated, and this is reflected in the curves (b1) and (b2) in Figs. 28 and 29. Losses in the conductor discs are proportional to clearance from the magnet discs and this may have shifted during the operation and later resetting of the ASCS. However, the overall temperature rises are similar to those observed in the 50hp unit and present no particular problems. Again the pump load characteristic is seen to impose a greater duty, and hence higher temperature rise on the conductor discs in particular.

4.4 New 200hp Motor

Again a brand new, NEMA 841, 4-pole induction motor was used for the 200hp tests. The data obtained is presented in Appendix 9.B – Sets 10 and 11. The following observations are made from those test records.

4.4.1 Speed and Torque

The target values for torque, for direct coupled operation, and for speed and torque for ASCS operation, were produced to a high degree of accuracy indicating good control of both the dynamometer and the ASCS.

4.4.2 Electrical Power Input and Utilization

Figs. 30 and 31 show the input power reductions that are possible through the use of the ASCS compared to directly coupled and throttled operation. The overall percentage reductions and form of the curves are very similar to those for the 50hp and 100hp units.

4.4.3 Power Factor and THD

The power factor levels and total harmonic distortion levels and the effects of the ASCS compared to direct coupling are in keeping with the results for the 50hp and 100hp units. No problems are seen in this area; power factor and THD levels are slightly better for this larger motor.

4.4.4 Sound Levels

The sound levels observed for the 200hp systems, direct coupled and ASCS coupled, are very similar to the corresponding levels recorded for the 100hp systems. Thus, approximately 10 dBA rise over a 77 dBA base is observed for the use of the ASCS.

4.4.5 Vibration

The observed vibration levels are small and present no problem.

4.4.6 Motor Temperatures

The temperature rises above ambient of the motor shaft-end bearing, for both direct coupled and ASCS operation are presented in Figs. 32 and 33 for fan loads and pump loads respectively. Here, contrary to expectations it is found that

the bearings of the motor appear to run cooler for ASCS operation. This is opposite to the findings for the 50hp motors and the 100hp motor.

It is believed that the differences in these findings is due to two causes. First, with the exception of the old 50hp motor, the three motors used in the test program were received directly from the manufacturer and were not operated at all before this test program. It is generally known that new motors exhibit higher bearing losses for several hours of operation until their conditions stabilize and the bearing grease takes on a more fluid form. Second, the 200hp motor was from a different manufacturer than the new 50hp and new 100hp motors. This 200hp motor is constructed with roller bearings rather than ball bearings as used in the 50hp and 100hp motors. The roller bearings are specifically designed to operate with lateral loads (normally for belt drives) such as is imposed by the mass of the ASCS.

The overall result of the tests, however, is that motor bearing temperature rise should not be a problem with the ASCS.

4.4.7 ASCS Temperatures

The temperature rises observed on the magnet discs of the 200hp ASCS are a little higher, for both fan and pump loads, than was observed for the 50hp and 100hp. However, at the level presented in Fig. 34 no problems are envisioned. However, the temperatures observed on the conductor discs were a matter of some concern.

Because the temperature rise of the 200hp conductor discs was so large it is necessary to present the data on a different scale to that used for the magnet discs. Consequently the format of presentation of the 200hp has been changed: magnet disc data, for both fan and pump operation, is given in Fig. 34 and conductor disc data, for both fan and pump operation is given in Fig. 35.

For fan and pump operations the hottest conductor disc was observed to have a maximum temperature rise of approximately 200°C and 260°C respectively. Clearly both these temperatures were indicative of inadequate heat dissipation from the discs. It is believed that this problem may also be

exacerbated by the substantial difference in the clearance of the gaps between the magnet disc and conductor disc on the two sides of the ASCS as shown in Fig. 36 (a). The discs of the ASCS had a mat black paint finish. The temperatures experienced caused blistering, flaking and eventually shedding of the paint as shown in Fig. 36 (b).

4.5 Reduction of Thermal Problem

The heat dissipation from the 50hp and 100hp ASCS units appears to be quite adequate. However the 200hp unit, in its original form, overheated substantially. To rectify this situation, heat sinks were added to the exterior surfaces of the conductor discs as shown in Fig. 11 (b). Sinks with both radially orientated and tangentially orientated fins were tried. Both were very successful in reducing the maximum temperature rise observed from over 260°C to approximately 100°C. With radial fins a substantial increase in sound level and a small but finite difference in input power level was observed: these were reduced to sound increases of only 2 to 3 dBA and a few watts of input power with tangential fins. In order to ensure that the reduced temperature levels were authentic, and that the addition of the fins had not shifted the maximum temperature to another flow rate condition, several data points were taken to ensure that maximum temperatures had been observed. The peak values are compared with the corresponding data for pump drive operation in Fig. 37. Thus the use of cooling fins is necessary for this largest ASCS tested and tangentially oriented vanes are preferred.

4.6 Starting Currents

As is well known, when starting direct-on-line (DOL), induction motors draw very large currents. Before the introduction of high efficiency motors a typical induction machine was expected to draw a starting current of approximately 600% of the full-load rated current. For high efficiency motors this ratio can now get as high as 1000%. This presents two problems to plant operators. First, switchgear relaying must be set to accommodate these starting current levels and second, allowances must sometimes be made to allow these currents to flow for substantial times when starting loads of high inertia. Of particular concern in high inertia load starting is the extremely large rotor

currents which can cause thermal damage. In certain cases this necessitates the use of over sized or conservatively rated motors: i.e. the motor may be sized on its thermal capability for starting rather than its load rating. Alternatively, to overcome these problems reduced voltage starting, or "soft-starters", are employed. A soft-start capability is inherently included in most VFDs.

The ASCS has the capability of decoupling the load from the driving motor during start. In some cases this will enable the motor to start virtually unloaded and then to have a high inertia load applied gradually after the motor has achieved normal operating speed. This was simulated in the laboratory. Fig. 38(a) shows the starting current of the 200hp motor coupled to the unloaded dynamometer: the high starting currents are drawn for approximately 20 millisecs. Fig. 38(b) shows the starting of the same motor which is initially disconnected from the dynamometer by the ASCS. The high starting currents flow for only 10 millisecs, hence reducing the thermal stress on the rotor in particular.

The tests described in Sections 4.5 and 4.6 were not part of the original job description and test plan. They were substituted for the duplicated VFD tests of the 200hp system.

5. VFD Test Results

The application of variable frequency drives (VFDs) in commercial and industrial facilities is increasing due to improved efficiencies leading to energy savings, as well as increased process control. Fig. 4 (b) shows schematically how VFDs are used to control fan and pump flows. The three VFDs tested (50kVA, 100kVA and 250kVA) were from a major manufacturer and were installed at the input of the appropriately rated induction motor as shown in Fig. 5. Note that a 250kVA VFD was used with the 200hp motor due to availability. The VFDs were connected directly to the laboratory 460V service, which again is maintained at rated value and fully balanced by the autotransformers shown in Fig. 5.

As with the testing of the ASCS described in the previous section, the torque-speed requirements given in Tables 3 (fan) and 4 (pump) for the adjustable speed systems were used with the testing of the VFDs. These performance points were required for the dynamometer to simulate adjustable speed operation, and were set as follows. The required operating speed was set by the VFD (controlled by the fundamental output frequency on the control panel), and then the torque corresponding to the required speed was set with the dynamometer. Having established a specific speed and torque condition, the system was left to operate in steady-state condition until all performance variables had stabilized. The following parameters of operation were then recorded:

(a) speed and torque (required values);
(b) VFD output frequency;
(c) electrical input voltage, current, power, true power factor (including harmonic distortion components), and total harmonic distortion (THD) of both voltage and current;
(d) sound levels at 20 ft from the test bed;
(e) vibrations, as the horizontal vertical and axial acceleration, at the drive motor bearing;
(f) ambient and motor temperatures.

To serve as a cross-check for errors or operational problems the tests were repeated. Consequently two data sets are given in Appendix 9.B for each of the tests, with the exception of the 200hp case. Only one data set was taken with the 250kVA VFD, in exchange for the additional thermal tests and the de-coupled run-up test, as described in Sections 4.5 and 4.6.

Fig. 39 shows the common VFD system topology. From left to right, is the source voltage, system impedance and then the input to the VFD which typically consists of a diode rectifier bridge to convert the ac input voltage to dc. On the dc-link there is a filter capacitor to minimize the voltage ripple, and the possibility of a dc-link inductor (can be specified). The dc-link inductor can serve to improve the dc voltage ripple to prolong the life of the capacitor, as well as reduce the input current harmonics. The dc-

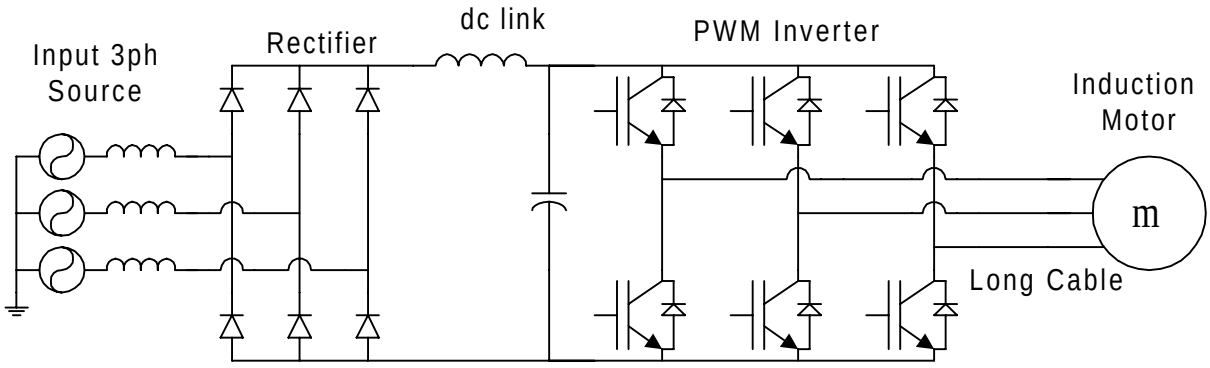

Fig. 39 Conventional Variable Frequency Drive (VFD) System.

link supplies the pulse-width modulated (PWM) inverter that supplies variable frequency voltages to the ac motor for speed control.

As mentioned in the introduction, the VFD diode rectifier front-end draws nonsinusoidal currents rich in odd harmonics. For rectifier systems supplied by balanced utility voltages, the input current characteristic harmonics are determined by:

$$h = kq \pm 1 \qquad (1)$$

where

h = order of the harmonics

k = 1,2,3,4,...,

q = number of pulses of the rectifier system

Conventional VFDs as shown in Fig. 39 have "six-pulse" rectifiers (q = 6), defined by the fact that the dc-bus voltage consists of portions of the line-to-line ac waveform and repeats with a 60° duration, i.e. containing six pulses in 360°. Therefore the characteristic harmonics present in the VFD input will be 5^{th} (300 Hz), 7^{th} (420 Hz), 11^{th} and 13^{th} etc. Under the conditions of utility voltage unbalance, the input current harmonics are not restricted to the converter characteristic harmonics of eqn. (1), and for example lower order 3^{rd} harmonic can appear. The problems associated with harmonics are well known [9] and include equipment heating and excess losses, mechanical oscillations in line driven machines, solid-state equipment malfunctioning and premature tripping due to interference, as well as the potential for overvoltages and excessive currents in networks due to resonance at the harmonic frequencies.

Additional VFD application issues have surfaced in recent years on the motor/load side of the system due to the high frequency operation of the PWM inverter. Switching frequencies of 2 to 20 kHz are common with insulated gate bipolar transistor (IGBT) technology for power levels up to 800 kW. However, the high rate of voltage rise (dv/dt) of 6000V/μs (typical for IGBT inverters) has adverse effects in the form of motor insulation stress, electromagnetic interference (EMI) and bearing and leakage

currents caused by common mode voltages [3]. In response to these concerns, a variety of mitigation techniques have been suggested as documented in [3], however these are still considered “band-aids” to problems that should be corrected inside the VFD, which would currently drive up the cost substantially.

Finally, VFDs can be more susceptible to power quality disturbances such as voltage sags, swells, transients (e.g. due to capacitor switching) and momentary interruptions (outages). VFD trips can result in a significant loss in revenue and costly down time for critical continuous processes.

5.1 New 50hp Motor

For the testing of the 50kVA VFD, a new 50hp, NEMA 841 standard, 4-pole induction motor from a major manufacturer was used. The data sets for baffled fan and throttled pump operation are given in Appendix 9.B – Set 4 (a) and (b), for comparison purposes. The corresponding data sets for VFD control are given in Appendix 9.B – Sets 12(a).1 and 12(a).2, and Sets 12(b).1 and 12(b).2. The following observations are made from the direct comparison of data Sets 4 and 12.

5.1.1 Speed, Torque and VFD Output Frequency

The VFD controlled the motor speed at the target speeds for both fan and pump operation, set by the VFD fundamental output frequency parameter on the control panel. The measured (test) torque conditions also met the required values to a highly acceptable level.

5.1.2 Electrical Power Input and Utilization

To compare overall system process efficiency between baffled, throttled and VFD control, the input power as a function of flow is compared. These are shown in Figs. 40 (fan) and 41 (pump). At 100% flow the baffles and throttle valves will be completely open, whereas the VFD will still be exhibiting some operational losses (namely switching), and therefore the VFD process will operate

at a slightly lower efficiency. However, as the % flow decreases, substantial savings for VFD operation are demonstrated.

5.1.3 Power Factor and THD

The power factor of the VFD input is significantly lower than that during baffled and throttled operation. This is to be expected because true power factor is measured, including the harmonics drawn by the VFD rectifier front-end as described at the beginning of this section.

The THD of the input currents of the VFD is significantly higher than during baffled and throttled operation, and can create potential harmonic problems as described in the beginning of this section. Fig. 42 shows example time domain waveforms of the voltage and current at the torque-speed operating point of 201N and 1697 r/min. The input current is very non-sinusoidal and rich in odd harmonics (5^{th}, 7^{th}, 11^{th}, 13^{th} etc.).

5.1.4 Sound Levels

Sound levels for VFD operation decrease as the motor speed is reduced as is expected. As is also expected, the sound levels with throttled control increase with decreased % flow, thus are inversely proportional to VFD operation. The dB range for the different systems are very comparable and vary from 75 to 77 dB.

5.1.5 Vibration

The measured accelerations at the motor are similar when using the VFD compared to the throttled Omega coupling operation. Specifically, the VFD levels are slightly lower, namely at reduced load, except at resonant points where the levels become slightly higher. Resonant frequencies/speeds can occur in mechanical loads. None of the levels measured are a cause for concern, and VFDs can be programmed to avoid these resonant points.

5.1.6 Motor Temperatures

As expected, with VFD operation, the motor temperatures increase with decreasing motor speed due to reduced self cooling effectiveness. However, the motor temperature is still comparable to the throttled case and does not present any concerns. In the throttled data sets, the motor temperatures for set 2 are lower than for set 1 because the brand new motor was still being "worked in" during data set 1 and therefore data set 2 is more accurate. Also note that in the VFD data set 2, there was a motor temperature recording error.

5.2 Old 50hp Motor

The set of tests described in Section 5.1 was repeated using an old, repaired, 50hp 4-pole motor, which will provide an assessment of the 50kVA VFD performance with motors other than new, high efficiency models,. The data sets for baffled fan and throttled pump operation are given in Appendix 9.B – Set 6 (a) and (b). The corresponding data Sets for ASCS control are given in Appendix 9.B – Sets 13(a).1 and 13(b).2. The following observations are made from the direct comparisons of data Sets 6 and 13, and also with Sets 4 and 12.

5.2.1 Speed, Torque and VFD Output Frequency

With the old 50hp motor, the VFD once again controlled the motor speed at the target speeds for both fan and pump operation, set by the VFD fundamental output frequency parameter on the control panel. The measured (test) torque conditions also met the required values to a highly acceptable level.

5.2.2 Electrical Power Input and Utilization

The efficiency of the VFD process with the old motor was always lower than that of the new motor under corresponding conditions. The differences range from approximately 1 to 7 percentage points. The efficiencies of the throttled and baffled loads were also always lower, with a range of 2 to 7 percentage points. The comparisons of input power as functions of flow are given in Figs. 43 and 44.

5.2.3 Power Factor and THD

The overall trends of power factor and THD as a function of flow rate for both VFD and throttling operation were very similar for the old 50hp as for the new 50hp discussed in Section 5.1.3. Generally, the old 50hp motor under VFD control has slightly lower power factors and higher THDs for given operating points when compared to the new 50hp VFD motor process. The VFD input current is again rich in odd harmonics with a time domain waveform similar to Fig. 41.

5.2.4 Sound Levels

Sound levels for VFD operation with the old 50hp motor are 1 to 3 dB higher than with the new 50hp motor (now ranging from 76 to 81 dB). The dB levels of the throttled processes with the old 50hp motor increased in a similar fashion and now range from 80 to 82 dB.

5.2.5 Vibration

With the old 50hp motor, the measured accelerations at the motor are generally slightly higher than compared to the new 50hp motor. In comparison with the throttled Omega coupling operation, the VFD operation again results in slightly lower vibration levels as the load is reduced. As with the new 50hp VFD operation, resonant points exist where the levels become slightly higher, though for the two processes (new and old) the resonance exists at different frequencies. Again, none of the levels measured are a cause for concern.

5.2.6 Motor Temperatures

The motor temperatures for the old 50hp motor under VFD control were 10°C to 20°C lower than for the new 50hp motor conditions. In comparison with the throttled operation, the old 50hp motor VFD process operates at 15°C lower at full speed, but as the temperatures increase with decreasing motor speed, ends up operating at 7°C higher at the lowest load point.

5.3 New 100hp Motor

The 100hp motor used with the 100kVA VFD was a new NEMA 841, 4-pole induction motor from a major manufacturer. The data obtained from these VFD tests are given in Appendix B: Set 14(a) and 14(b) for the fan and pump operation, and these will be compared with Set 8(a) and (b) for baffled fan and throttled pump operation. The following observations are made from data Sets 8 (throttled) and 14 (VFD) and the corresponding input power vs. flow graphs.

5.3.1 Speed, Torque and VFD Output Frequency

The VFD controlled the motor speed at the target speeds for both fan and pump operation, set by the VFD fundamental output frequency parameter on the control panel. The measured (test) torque conditions also met the required values to a highly acceptable level.

5.3.2 Electrical Power Input and Utilization

The VFD input power as a function of flow is compared in Figs. 45 (fan) and 46 (pump) against baffled and throttled processes. Again, as the % flow decreases, power reductions resulting in substantial savings for VFD operation are demonstrated. Power reductions are slightly greater for pump operation than for fan operation.

5.3.3 Power Factor and THD

The power factor of the VFD input is again lower than during baffled and throttled operation, as expected due to the high harmonic content in the input current, as found in Sections 5.1.3 and 5.2.3.

The THD of the input currents of the VFD is also significantly higher than during baffled and throttled operation. The input current will have the same waveshape as that shown in Fig. 42. The higher the kVA rating of the VFD load, the higher the magnitude of harmonics that will be injected into the system, and

thus the higher the risk of harmonic problems as discussed in the beginning of this section.

5.3.4 Sound Levels

As in Section 5.1.4, the dB range for the VFD and throttled systems are comparable and vary from 75 to 78 dB.

5.3.5 Vibration

The measured accelerations at the motor are similar when using the VFD compared to the throttled Omega coupling operation. In general, the vibration levels under 100kVA VFD operation are slightly lower than under throttled operation.

5.3.6 Motor Temperatures

With VFD operation, the motor temperatures increase with decreasing motor speed, from slightly below the throttled condition temperature at full speed, to 5°C above the throttled temperature at the lowest speed/load point.

5.4 New 200hp Motor

For the 200hp tests, a new NEMA 841, 4-pole induction motor was controlled by a 250kVA VFD (a 200kVA VFD was not available). The effect of the overrated VFD on the performance comparison with the throttled operation is negligible. The data obtained is presented in Appendix 9.B – Set 15, as well as Figs. 47 and 48. The following observations are made from those test records.

5.4.1 Speed, Torque and VFD Output Frequency

The VFD controlled the motor speed at the target speeds for both fan and pump operation, set by the VFD fundamental output frequency parameter on the control panel. The measured (test) torque conditions also met the required values to a highly acceptable level.

5.4.2 Electrical Power Input and Utilization

The 250kVA VFD input power as a function of flow is compared in Figs. 47 (fan) and 48 (pump) against baffled and throttled processes. Again, as the % flow decreases, power reductions resulting in substantial savings for VFD operation are demonstrated. As with the 100kVA VFD, power reductions are slightly greater for pump operation than for fan operation.

5.4.3 Power Factor and THD

The power factor of the VFD input is again lower than during baffled and throttled operation, while the THD is significantly higher, yielding similar results as for the 50kVA and 100kVA VFDs.

5.4.4 Sound Levels

The dB range for the VFD is 2 to 3 dB higher than the throttled systems at high motor speeds, and equivalent at low speeds.

5.4.5 Vibration

The measured accelerations at the motor are similar when using the VFD compared to the throttled Omega coupling operation. In general, the vibration levels under 200kVA VFD operation are slightly lower than under throttled operation.

5.4.6 Motor Temperatures

Again, with VFD operation, the motor temperatures increase with decreasing motor speed, from slightly below the throttled condition temperature at full speed, to 5°C above the throttled temperature at the lowest speed/load point under 200kVA operation.

6. Interpretation for Applications

6.1 Basic Physical Considerations

Before a decision is made to install an ASCS in a particular application certain practical issues need to be addressed. For the most part these are relatively obvious such as the following points.

(i) The ASCS requires more space between motor and load than a direct fixed mechanical coupling; can this space be accommodated in the plant?

(ii) The ASCS has a larger diameter than the equivalent mechanical coupling; can this be accommodated and does this present an additional or increased safety consideration? If the latter point is valid, should a protective cover be installed and will this affect the cooling of the ASCS and its effective rating? The rating of the ASCS units will be addressed in Section 6.3.

(iii) If the ASCS can be economically justified compared to throttling control or VFD application the changed provision for controls must be determined. It should be emphasized here that the ASCS operates in situ in the plant whereas VFDs are usually located in a remote climate controlled room which could be a considerable cost factor.

(iv) Although the ASCS is shown to reduce the losses involved in flow control, compared to baffles and throttling valves, the losses are now concentrated in the area between the motor and the load rather than being distributed elsewhere about the plant. Could this be a problem in areas where the ambient temperature is already high?

6.2 Economic Considerations

The prime issue to be addressed in the potential application of an ASCS is almost certainly economic: i.e., if an ASCS is to be installed in an application in which the flow is currently controlled by baffles or throttling valves, what is the payback period? This is similar to the issues facing the application of VFDs and this has been successfully developed into a piece of applications software, ASDMaster [2] by EPRI/ASDO. To enable similar decisions to be made for ASCS it would be valuable for comparable software to be developed here also.

At the basis of the payback issue is the determination of energy savings and the data presented in Section 4 can provide some of the answers to this. Figs 49 and 50 consist of a composite of the test data presented in Figs. 12, 18, 24, 30 and 40, 43, 45, 47 for fan operation, and Figs. 13, 19, 25, 31, and 41, 44, 46, 48 for pump operation. In Figs. 49 and 50 the power requirements have all been rationalized to 100hp: i.e., the 50hp motor data is multiplied by 2 and the 200hp data is divided by 2. From these composites it is evident that, regardless of the manner of flow control (throttled, ASCS, or VFD) the order of system efficiency is 200hp, 100hp, new 50hp and old 50hp. This is in keeping with general rules of thumb: bigger is more efficient in induction machines (both the motor and the ASCS are induction devices); an older, repaired motor will be less efficient than a new one. Also evident from Figs 49 and 50 is that the difference between the adjusted (scaled) power levels is very small. Consequently it is justifiable to develop single characteristics for the energy savings available from the ASCS applications, expressed in percentages, as functions of flow. Figs 51 and 52 are per unit power savings characteristics, for the fan and pump respectively, determined from

$$\text{power savings, \%} = \frac{\text{power rquirement throttled} - \text{power requirement ASCS}}{\text{full load power rating}}$$

From these two figures the savings in operating costs due to reduced energy utilization can be calculated from

$$\Delta\$ = \sum \Delta P_f \times t_f \times R$$

In which

ΔP_f = the per unit power savings for flow rate f from Figs 51 or 52

t_f = the time, in hours, for which the flow rate f is required

R = the peak rating of the system in kW (e.g., 74.6 for 100 hp fan pump)

Σ indicates a sum of the product for all the identified time periods (per month, say)

This formula can then be applied to determine the time to reach economic payback for the application of the ASCS.

A particular caveat should be noted at this point. The characteristic of Fig 51 is generally applicable to all fan loads, which can be assumed to have torques proportional to the square of speed and powers proportional to the cube of speed. However, Fig 52 is not so generally applicable to all pumps but here can only serve as an approximate guide. This is based on the nature of the load of a pump which has two components: the flow component, which is comparable to the fan load of power proportional to the cube of speed; the static head component, in which power is directly proportional to speed. The effects of these components, and their relationship to the rating of the ASCS is addressed in the next section.

6.3 ASCS Rating

In order to complete the economic viability or payback calculation discussed in the proceeding section it will be necessary to compare the energy (and dollar) savings with the capital (and installation and maintenance) cost of the ASCS. The capital cost of the ASCS will depend on the rating of the unit recommended for a particular application. The size of the required ASCS depends on its ability to dissipate the losses that are produced in its conductor disks while maintaining temperatures that are within safe bounds for the materials being used. As was emphasized in Section 2, the losses in the ASCS are dependent on two major factors: the slip at which the ASCS is operating; the nature of the power requirement of the load, as a function of speed (or slip).

6.3.1 Fans and Very Low Head Pumps

For these applications:

$$T = K_1 S^2$$

$$P = K_1 S^3$$

and $$L = K_1 S^3 (1 - S_{pu})$$

in which: K_1 is a constant depending on the fan size and construction; S is the speed of the fan in radians/sec; T is the torque in Nm; P is the power in kilowatts; L is the loss in the ASCS in kilowatts. S_{pu} is the per unit speed given by

$$S_{pu} = \frac{S_{\max} - S_{load}}{S_{\max}}$$

In which: S_{max} is the max speed of the driving motor at required load (approximately the motor synchronous speed); S_{load} is the speed of the load at the condition under consideration.

6.3.2 High-Head, Very Low Flow, Pumps

For these applications

$T = K_2$

$P = K_2S$

$L = K_2S\ (1 - S_{pu})$

6.3.3 Intermediate Head, Appreciable Flow, Pumps

$T = K_1S^2 + K_2$

$P = K_1S^3 + K_2S$

$L = (K_1S^3 + K_2S)(1 - S_{pu})$

For a particular application the loss characteristic needs to be determined to ensure that the maximum loss point (10.5% of rating for pure fan load as shown in Fig 3) does not exceed the allowable losses of the ASCS.

7. Conclusions and Recommendations

7.1 Conclusions of Test Program

7.1.1 The tests have demonstrated the viability of the principle of the ASCS as a simple, non-electronic, adjustable-speed drive.

7.1.2 The ASCS units tested were prototypes and certain features still need attention as will be addressed in Section 7.2

7.1.3 The ASCS has demonstrated its potential to reduce energy consumption for fans and pumps compared to flow control by baffles and throttling valves. The power reduction is shown in Figs. 51 and 52 to be up to 30% for a fan and up to 44% for a pump.

7.1.4 The power reductions observed by use of the ASCS are less than that obtained by use of a VFD, as shown in Figs. 49 and 50. Typically, for a fan load, the power reduction is between 50% and 80% (with an average of 65%) of the power reduction obtained by the VFD. For the pump load tested, the power reduction is between 50% and 70% (with an average of 62%) of the power reduction obtained by the VFD.

7.1.5 At higher flow rates the power factor of a motor driving a load via an ASCS is virtually the same as for a mechanically coupled motor with flow controlled by baffles and throttling valves. At low flow rates the off-loading of the ASCS causes the power factor to be substantially lower. When compared to the VFD, the ASCS has better power factor at high loads but lower power factor at low loads as shown in Fig. 53. It should be noted, however, that the low power factors experienced by use of ASCS are more readily correctable. The ASCS power factor is due almost entirely to displacement of voltage and current, whereas the VFD power factor is dictated for the most part by distortion (harmonic content) of the current.

7.1.6 The total harmonic distortion (THD) experienced by use of the ASCS is comparable to directly coupled motors. The THD of VFDs is very poor compared to the ASCS as shown in Fig. 54, due to the operation of the diode rectifiers. Correction of the THD for VFDs is significantly expensive.

7.1.7 The sound levels experienced by use of ASCS are slightly higher than for directly coupled motor systems, probably due to the windage of the ASCS itself. The VFD, in contrast, results in lower sound levels particularly as the speed reduces

7.1.8 Vibration levels do not seem to be an issue with ASCS applications, however the test program did not rigorously address the issues of possible torque pulsations and vibrations issuing from the load. Certainly the ASCS is not a source of pulsations which has been a problem with some VFDs. These problems of VFD generated vibrations have mostly been resolved by design.

7.1.9 Motor temperatures are a complex issue and are a function of heat from several sources. The data indicates that the shaft-end bearing is likely to be hotter with the ASCS due to the losses from the conductor plates, though this is not always the case and temperature differences do not appear significant. Motor losses and motor cooling are improved with ASCS control compared to both throttle and VFD control. For operation with throttling systems the motor is always running at a higher load and hence produces more losses. For VFD operation the self cooling of the motor is reduced as the speed is reduced. For constant torque loads this becomes a problem requiring supplemental forced cooling. However for fans and pumps this may not be necessary.

7.1.10 It is essential that the magnet discs of an ASCS do not approach the curie temperature of the magnetic alloys employed. For the loads that were driven in this study this was never a problem. The highest magnet disc temperature rise observed was in the region of 40° C which leaves significant safety margin even in a 40° C ambient.

7.1.11 The temperature rise of the conductor discs is a more significant problem. Fig. 55 shows the correlation between the theoretical conductor disc losses and the measured temperature rise of the 100hp ASCS. The slight off-set of the latter is probably due to the effect of reduced cooling with decreasing ASCS speeds. The peak temperature rises increase with increasing ASCS rating as given in the following table.

Table 5 - Temperature Rise of ASCS Conductor Discs

Rating hp	50 New	50 Old	100	200	200 radial finned	200 tangential finned
Fan Load: Temp. Rise °C	70	70	80	200	NA	NA
Pump Load Temp. Rise °C	75	80	92	260	≈100	≈100

7.1.12 The temperature rises given in Table 5 are for low static head systems. As the static head increases there is an increasing component of constant torque across the speed (flow) range. This will produce a more troublesome and higher loss profile.

7.1.13 The ASCS enables speed control without several problems associated with the use of VFDs: bearing currents due to common-mode voltages; insulation stress due to high frequency voltage reflections at motor terminals; interference with data acquisition and control equipment (EMI); current harmonic pollution of the supply.

7.1.14 The ASCS will probably be less susceptible than VFDs to power quality disturbances such as voltage sags, and will tend to respond in a similar fashion as the stand alone motor.

7.2 Recommendations

The MagnaDrive couplings evaluated in this study were pre-production prototypes and, as such will not represent the final marketable equipment. Before production designs are finalized it is recommended that the following issues receive attention.

7.2.1 The applications of ASCS need to be carefully controlled to promote the use only for loads having rapidly decreasing torque requirements as a function of speed.

7.2.2 The installation and set-up process needs to become less critical than that observed in this test program. The units tested appeared to need very special attention during installation which is not appropriate for widespread industrial use.

7.2.3 The problem of cooling of the conductor discs needs to be addressed, particularly if larger units are to be constructed. A thermodynamic analysis, maybe using finite element techniques, will be worthwhile to ensure that the cooling provisions are adequate but not unduly expensive.

7.2.4 A magnetic field system analysis would be worthwhile to ensure that major variables such as copper thickness, magnet size and steel thickness are within reasonable bounds.

7.2.5 Dynamic effects, during acceleration and decelleration and torque pulsations need to be investigated. The breakdown torque of the ASCS needs to be established and made a part of the specification.

8. References

1. EPRI/Bonneville Power Administration “Electric Motor Systems Sourcebook” Report #RP3087-21, February 1993.
2. EPRI/Adjustable Speed Drive Demonstration Office, “ASD Master”, 1996.
3. A. von Jouanne, H. Zhang, A. Wallace, “An Evaluation of Mitigation Techniques for Bearing Currents, EMI and Over-Voltages in ASD Applications”, IEEE Trans. on Industry Applications, Sept./Oct. 1998, pp. 1113-1122.
4. J. C. Conzett, J. D. Robechek, “Adjustable Speed Drives as Applied to Centrifugal Pumps”, Pacific Energy Association Pump Workshop, Long Beach, CA, January 6-7, 1981.
5. US Department of Energy – Bonneville Power Association, “Testing and Evaluation of the MagnaForce Adjustable Coupling”, Report #DOE/BPA 13314-1, June 1995.
6. A. Wallace, C. Wohlgemuth, and K. Lamb, “A High Efficiency, Alignment and Vibration Tolerant, Coupler Using High Energy-Product Permanent Magnets”, IEE Seventh International Conference on Electrical Machines and Drives, Publication # , 1995, pp232 – 236.
7. Rexnord Corporation, “The Future of Power Transmission is Here!”, Rexnord Bulletin No. 4500, 1997.
8. A. C. Smith, S. Williamson, A. Benhama, L. Counter and J. M. Papadopoulos, “Magnetic Drive Couplings”, IEE Ninth International Conference on Electric Machines and Drives, Publication No. 468, 1999, pp 232 – 236.
9. D. E. Rice, “Adjustable Speed Drive and Power Rectifier Harmonics – Their effect on Power Systems Components”, IEEE Transactions on Industry Applications, vol. IA-22, no. 1, 1986, pp. 161-177.

9. Appendices

9.A Equipment Specifications

9.A.1 The Dynamometer System

	Machine	Converter
Model	1K 447THDN4038 AA-W	MD-300
Manufacturer	Marathon Electric Co. Wausau, WI	Kenetech Windpower Livermore, CA
Volts	460	480
Current, full load Amps	332	350
Horse Power	300	300
r/min; Hz	0 to 4,000	0 to 135
Poles/phases	4	3
Duty	Cont.	Cont.
Serial Number	41890480-9/16	001

9.A.2 Torque and Speed Measurement System

Model	1804-10K and 1804-5K transducers 7530-115 signal conditioner and readout
Manufacturer	Eaton Corporation – Lebow Products 1725 Maplelawn Road PO Box 1089 Troy, MI 48099
Torque Rating	10,000 lb-in and 5,000 lb-in
Nonlinearity	± 0.05% of full scale
Nonrepeatability	± 0.025% of full scale
Hysteresis	0.05% of full scale
Temp. Compensated	70°F to 170°F
Speed Range	0-27,000 r/min – accuracy better than 1/10 r/min
Definition	60 pulses per rev
Error	< 1 count per sec

9.A.3 Measurement of Input Currents, Voltages, Real Power, Apparent Power, Reactive Power, Power Factor

	Specified Accuracy	
	DC and 45 Hz to 450 Hz	0.1 Hz to 500kHz
Voltage and Current	0.05% reading +0.05% range	0.10% reading +0.05% range
Power, VA, and VAR	0.01% reading +0.1% range	0.2% reading +0.1% range

Set 1

Set 2

Set 3

Set 4(a)

Set 4(b)

Set 5(a)1

Set 5(a)2

Set 5(b)1

Set 5(b)2

Set 6(a)

Set 6(b)

Set 7(a)1

Set 7(a)2

Set 7(b)1

Set 7(b)2

Set 8(a)

Set 8(b)

Set 9(a)1

Set 9(a)2

Set 9(b)1

Set 9(b)2

Set 10(a)

Set 10(b)

Set 11(a)1

Set 11(a)2

Set 11(b)1

Set 11(b)2

Set 12(a)1

Set 12(a)2

Set 12(b)1

Set 12(b)2

Set 13(a)1

Set 13(a)2

Set 13(b)1

Set 13(b)2

Set 14(a)1

Set 14(a)2

Set 14(b)1

Set 14(b)2

Set 15(a)1

Set 15(a)2